

PLANE WAVE DISCONTINUOUS GALERKIN METHODS FOR THE HELMHOLTZ EQUATION AND MAXWELL EQUATIONS IN ANISOTROPIC MEDIA *

LONG YUAN [†] AND QIYA HU [‡]

Abstract. In this paper we are concerned with plane wave discontinuous Galerkin (PWDG) methods for Helmholtz equation and time-harmonic Maxwell equations in three-dimensional anisotropic media, for which the coefficients of the equations are matrices instead of numbers. We first define novel plane wave basis functions based on rigorous choices of scaling transformations and coordinate transformations. Then we derive the error estimates of the resulting approximate solutions with respect to the condition number of the coefficient matrices, under a new assumption on the shape regularity of polyhedral meshes. Numerical results verify the validity of the theoretical results, and indicate that the approximate solutions generated by the proposed PWDG method **possess high accuracy**.

Key words. Helmholtz equation, time-harmonic Maxwell's equations, anisotropic media, plane wave basis, error estimates.

AMS subject classifications. 65N30, 65N55.

1. Introduction. The plane wave method, which is based on the Trefftz approximation space made of plane wave basis functions, was first introduced to discretization of homogeneous Helmholtz equation and was then extended to discretization of homogeneous time-harmonic Maxwell's equations and elastic wave equations. Various examples of the plane wave methods has been systematically surveyed in [10], for example, the ultra weak variational formulation (UWVF) [1–3, 15, 16], the plane wave discontinuous Galerkin (PWDG) method [5–11], the plane wave least-squares (PWLS) method [12, 13, 20, 21, 27]. The plane wave least-squares combined with local spectral finite element (PWLS-LSFE) method was recently proposed in [14] for nonhomogeneous Helmholtz equation and time-harmonic Maxwell equations. The plane wave method has an important advantage over Lagrange finite elements for discretization of the Helmholtz equation and time-harmonic Maxwell equations [6, 10, 15]: to achieve the same accuracy, **relatively fewer degrees of freedom** are enough in the plane wave-type methods owing to the particular choice of the basis functions that **(possibly approximately)** satisfy the considered PDE without boundary conditions.

In [16] the UWVF method was first extended to discretization of homogeneous Maxwell's equations in anisotropic media. The studies in [16] were devoted to approximating the Robin-type trace of the electric and magnetic fields in an anisotropic medium, and focus on the numerical tests and convergence analysis in TM mode scattering, which can result in a Helmholtz equation in two dimensions with an anisotropic coefficient. **In addition, the work [16, 24, 25] proposed the anisotropic plane wave basis functions, based on a coordinate transformation, for two-dimensional anisotropic Helmholtz equations.**

It was pointed out in [16, p.351] that, for three-dimensional anisotropic time-harmonic Maxwell's system, *almost all theoretical questions related to the 3D UWVF approach to anisotropic media are still open: in particular, the relevant approximation properties of sums*

*The first author was supported by China NSF under the grant 11501529 and Qindao applied basic research project under grant 17-1-1-9-jch. The second author was supported by the Natural Science Foundation of China G11571352.

[†] College of Mathematics and Systems Science, Shandong University of Science and Technology, Qingdao 266590, China (yuanlong@lsec.cc.ac.cn).

[‡] 1. LSEC, Institute of Computational Mathematics and Scientific/Engineering Computing, Academy of Mathematics and Systems Science, Chinese Academy of Sciences, Beijing 100190, China; 2. School of Mathematical Sciences, University of Chinese Academy of Sciences, Beijing 100049, China (hgy@lsec.cc.ac.cn).

of anisotropic plane waves are not known. Meanwhile, the three-dimensional Maxwell equations in anisotropic media with positive definite matrices play an important role in practical physical applications (see [19, p. 5-6]). Recently, the PWDG method was applied to discretization of three-dimensional anisotropic time-harmonic Maxwell's equations with diagonal matrix coefficients [26], in which rough error estimates of the resulting approximate solutions were derived.

In this paper, we first study the PWDG method for three-dimensional Helmholtz equation and time-harmonic Maxwell equations in more general anisotropic media, where the coefficient of the equations is a positive definite matrix instead of diagonal matrix. In order to deal with such complicated models and build better convergence results, we have to carefully define plane wave basis functions by rigorous choices of the scaling transformations and the coordinate transformations. Besides, we propose a new assumption on the triangulation: the transformed triangulation $\hat{\mathcal{T}}_h$ rather than the physical triangulation \mathcal{T}_h is shape regular. Own to such an assumption, we can verify that the defined transformations have the desired stability estimates on the condition number of the anisotropic coefficient matrix, and further prove that the resulting approximate solutions have the desired convergence order with respect to the condition number of the coefficient matrix. Numerical experiments indicate that the approximate solutions generated by the proposed PWDG method possess high accuracy, and verify the validity of the theoretical results.

In order to clarify the novelty of the present paper, we would like to emphasize the differences with the existing works:

1) the models are different: in the present paper, we consider three-dimensional time-harmonic Maxwell's equations with general coefficients that are (constant) positive definite matrices, but in [26] three-dimensional time-harmonic Maxwell's equations with diagonal matrix coefficients were considered; in [16], three-dimensional time-harmonic Maxwell's equations that can be transformed into two-dimensional Helmholtz equations were studied; in [25, 24] two-dimensional Helmholtz equations with coefficients being positive definite matrices were studied.

2) the methods are different: in the present paper, we employ a new transformation $\hat{\mathbf{x}} = \Lambda^{-\frac{1}{2}} P \mathbf{x}$ that is different from the old transformation $\hat{\mathbf{x}} = A^{-\frac{1}{2}} \mathbf{x}$ that used in [16, 26, 25, 24]. Moreover, we propose a new assumption on the triangulation such that the transformed triangulation $\hat{\mathcal{T}}_h$ rather than the physical triangulation \mathcal{T}_h is shape regular.

3) the results are different: in the present paper, we obtained obviously better error estimates than the existing works, thanks to the proposed transformation.

The paper is organized as follows. In Section 2, we present PWDG method for the three-dimensional anisotropic Helmholtz equation and analyze the convergence of the proposed PWDG method. In Section 3, we extend the results obtained in Section 2 to the three-dimensional anisotropic time-harmonic Maxwell equations. Finally, we report some numerical results to confirm the effectiveness of the proposed method.

2. PWDG method for three-dimensional anisotropic Helmholtz equation. To our knowledge, there seems no work on plane wave method for three-dimensional anisotropic Helmholtz equation in literature. In this section we first introduce PWDG method for three-dimensional anisotropic Helmholtz equation.

2.1. The model and its variational formula. Consider the three-dimensional (3D) anisotropic Helmholtz equation of acoustic wave field u (refer to [17]):

$$(2.1) \quad -\nabla \cdot A \nabla u - \omega^2 u = 0 \quad \text{in } \Omega$$

with the Robin-type boundary condition

$$(2.2) \quad \mathbf{n} \cdot A \nabla u + i\omega u = g \quad \text{on } \gamma = \partial\Omega.$$

Here Ω is a bounded domain in three dimensions, \mathbf{n} denote the unit outer normal vector to the boundary $\partial\Omega$; A is a real-valued 3×3 matrix; $\omega > 0$ is the temporal frequency of the field and $g \in L^2(\partial\Omega)$. We assume that the matrix A is symmetric and positive definite.

We will derive a variational formula of the considered model based on a partition of the solution domain Ω (refer to [6]).

For convenience, assume that Ω is a polyhedron. Let Ω be divided into a union of some elements in the sense that

$$\bar{\Omega} = \bigcup_{k=1}^N \bar{\Omega}_k, \quad \Omega_l \cap \Omega_j = \emptyset \quad \text{for } l \neq j,$$

where each Ω_k is a polyhedron. Let \mathcal{T}_h denote the partition comprised of the elements $\{\Omega_k\}$, where h denotes the diameter of the maximal element in $\{\Omega_k\}$. Define

$$\Gamma_{lj} = \partial\Omega_l \cap \partial\Omega_j, \quad \text{for } l \neq j$$

and

$$\gamma_k = \bar{\Omega}_k \cap \partial\Omega \quad (k = 1, \dots, N), \quad \gamma = \bigcup_{k=1}^N \gamma_k.$$

We denote by $\mathcal{F}_h = \bigcup_k \partial\Omega_k$ the skeleton of the mesh, and set $\mathcal{F}_h^B = \mathcal{F}_h \cap \partial\Omega$ and $\mathcal{F}_h^I = \mathcal{F}_h \setminus \mathcal{F}_h^B$. Let u and $\boldsymbol{\sigma}$ be a piecewise smooth function and vector field on \mathcal{T}_h , respectively. On $\partial\Omega_l \cap \partial\Omega_j$, we define

$$(2.3) \quad \begin{aligned} & \text{the averages: } \{\{u\}\} := \frac{u_l + u_j}{2}, \quad \{\{\boldsymbol{\sigma}\}\} := \frac{\boldsymbol{\sigma}_l + \boldsymbol{\sigma}_j}{2}, \\ & \text{the jumps: } \llbracket u \rrbracket_N := u_l \mathbf{n}_l + u_j \mathbf{n}_j, \quad \llbracket \boldsymbol{\sigma} \rrbracket_T := \mathbf{n}_l \times \boldsymbol{\sigma}_l + \mathbf{n}_j \times \boldsymbol{\sigma}_j, \\ & \llbracket \boldsymbol{\sigma} \rrbracket_N = \mathbf{n}_l \cdot \boldsymbol{\sigma}_l + \mathbf{n}_j \cdot \boldsymbol{\sigma}_j, \end{aligned}$$

where \mathbf{n} denotes the unit outer normal vector on the boundary of each element Ω_k .

Define the broken Sobolev space

$$(2.4) \quad H^s(\mathcal{T}_h) = \{v \in L^2(\Omega) : v|_{\Omega_k} \in H^s(\Omega_k) \text{ for } \forall \Omega_k \in \mathcal{T}_h\}.$$

As usual, we assume that each entry in A is a constant. Let $V(\mathcal{T}_h)$ be the piecewise Trefftz space defined on \mathcal{T}_h by

$$(2.5) \quad V(\mathcal{T}_h) = \{v \in H^2(\mathcal{T}_h); -\nabla \cdot A \nabla v - \omega^2 v = 0 \text{ in each } \Omega_k \in \mathcal{T}_h\}.$$

Let α and β be two positive numbers, and let $\delta \in (0, \frac{1}{2}]$. Define the sesquilinear form $A_h(\cdot, \cdot)$ by

$$\begin{aligned} \mathcal{A}_h(u, v) &= \int_{\mathcal{F}_h^I} \{\{u\}\} \overline{\llbracket A \nabla_h v \rrbracket_N} dS + i\omega^{-1} \int_{\mathcal{F}_h^I} \beta \llbracket A \nabla_h u \rrbracket_N \cdot \overline{\llbracket A \nabla_h v \rrbracket_N} dS \\ &\quad - \int_{\mathcal{F}_h^I} \{\{A \nabla_h u\}\} \cdot \overline{\llbracket v \rrbracket_N} dS + i\omega \int_{\mathcal{F}_h^I} \alpha \llbracket u \rrbracket_N \cdot \overline{\llbracket v \rrbracket_N} dS \end{aligned}$$

$$(2.6) \quad \begin{aligned} & + \int_{\mathcal{F}_h^B} (1 - \delta) u \overline{(A \nabla_h v \cdot \mathbf{n})} dS + i\omega^{-1} \int_{\mathcal{F}_h^B} \delta (A \nabla_h u \cdot \mathbf{n}) \overline{(A \nabla_h v \cdot \mathbf{n})} dS \\ & - \int_{\mathcal{F}_h^B} \delta (A \nabla_h u \cdot \mathbf{n}) \bar{v} dS + i\omega \int_{\mathcal{F}_h^B} (1 - \delta) u \bar{v} dS, \quad \forall u, v \in V(\mathcal{T}_h). \end{aligned}$$

and

$$(2.7) \quad \ell_h(v) = i\omega^{-1} \int_{\mathcal{F}_h^B} \delta g \overline{(A \nabla_h v \cdot \mathbf{n})} dS + \int_{\mathcal{F}_h^B} (1 - \delta) g \bar{v} dS, \quad \forall v \in V(\mathcal{T}_h).$$

Then, for a given g , the variational problem associated with (2.1)-(2.2) can be expressed as follows (see [6, Section 2]): Find $u \in V(\mathcal{T}_h)$ such that

$$(2.8) \quad \mathcal{A}_h(u, v) = \ell_h(v), \quad \forall v \in V(\mathcal{T}_h).$$

We endow the space $V(\mathcal{T}_h)$ with the norm

$$(2.9) \quad \begin{aligned} \|v\|_{\mathcal{F}_h}^2 & := \omega^{-1} \|\beta^{1/2} \llbracket A \nabla_h v \rrbracket_N\|_{0, \mathcal{F}_h^I}^2 + \omega \|\alpha^{1/2} \llbracket v \rrbracket_N\|_{0, \mathcal{F}_h^I}^2 \\ & + \omega^{-1} \|\delta^{1/2} A \nabla_h v \cdot \mathbf{n}\|_{0, \mathcal{F}_h^B}^2 + \omega \|(1 - \delta)^{1/2} v\|_{0, \mathcal{F}_h^B}^2 \end{aligned}$$

and the augmented norm

$$(2.10) \quad \begin{aligned} \|v\|_{\mathcal{F}_h^+}^2 & := \|v\|_{\mathcal{F}_h}^2 + \omega \|\beta^{-1/2} \{\{v\}\}\|_{0, \mathcal{F}_h^I}^2 \\ & + \omega^{-1} \|\alpha^{-1/2} \{\{A \nabla_h v\}\}\|_{0, \mathcal{F}_h^I}^2 + \omega \|\delta^{-1/2} v\|_{0, \mathcal{F}_h^B}^2. \end{aligned}$$

As in [6], we can show the following existence, uniqueness and continuity of solution of the above variational problem.

LEMMA 2.1. *There exists a unique u solution to (2.8); moreover, we have*

$$(2.11) \quad \begin{aligned} & -\operatorname{Im}[\mathcal{A}_h(w, w)] = \|w\|_{\mathcal{F}_h}^2 \\ & \text{and } |\mathcal{A}_h(w, \xi)| \leq C \|w\|_{\mathcal{F}_h^+} \|\xi\|_{\mathcal{F}_h}, \quad \forall w, \xi \in V(\mathcal{T}_h). \end{aligned}$$

2.2. Discretization for the 3D anisotropic Helmholtz equation. Since A is positive definite matrix, there exists an orthogonal matrix P and a diagonal positive definite matrix $\Lambda = \operatorname{diag}(\lambda_{\min}, \lambda_{\text{mid}}, \lambda_{\max})$ such that $A = P^T \Lambda P$, where $\lambda_{\min} \leq \lambda_{\text{mid}} \leq \lambda_{\max}$ are constant and the superscript T denotes matrix transposition. Of course, we can assume that $\det(P) = 1$. It is clear that $A^{\frac{1}{2}} = P^T \Lambda^{\frac{1}{2}} P$. Define a coordinate transformation:

$$(2.12) \quad \hat{\mathbf{x}} = \Lambda^{-\frac{1}{2}} P \mathbf{x} \stackrel{\Delta}{=} S \mathbf{x}, \quad \hat{\mathbf{x}} = (\hat{x} \hat{y} \hat{z})^T, \quad S = \Lambda^{-\frac{1}{2}} P, \quad \mathbf{x} = (x y z)^T.$$

For convenience, we use p_1, p_2 and p_3 to denote three column vectors of P , and use q_1, q_2, q_3 to denote the three row vectors of P . Then each of these vectors is a three dimensional unit vector. Moreover, p_1, p_2 and p_3 (and q_1, q_2, q_3) are orthogonal each other. Set $u(\mathbf{x}) = u(S^{-1} \hat{\mathbf{x}}) \stackrel{\Delta}{=} \hat{u}(\hat{\mathbf{x}})$.

Let $\hat{\Omega}$ and $\hat{\Omega}_k$ denote the images of Ω and Ω_k under the coordinate transformation (2.12), respectively. Since the map S is linear, the transformed domain $\hat{\Omega}$ and elements $\hat{\Omega}_k$ are also polyhedrons. We use $\hat{\mathbf{n}}$ to denote the unit outer normal vector on the boundary of each element $\hat{\Omega}_k$, and $\hat{\mathcal{T}}_{\hat{h}}$ to denote the partition comprised by the elements $\{\hat{\Omega}_k\}$, where \hat{h} is the maximal diameter of the transformed elements $\{\hat{\Omega}_k\}$. Set $\hat{\mathcal{F}}_{\hat{h}} = \bigcup_k \partial \hat{\Omega}_k$, $\hat{\mathcal{F}}_{\hat{h}}^B = \partial \hat{\Omega}$ and $\hat{\mathcal{F}}_{\hat{h}}^I = \hat{\mathcal{F}}_{\hat{h}} \setminus \hat{\mathcal{F}}_{\hat{h}}^B$.

We denote by ∇_h and $\hat{\nabla}_h$ the element application of the gradient operator $\nabla = (\frac{\partial}{\partial x}, \frac{\partial}{\partial y}, \frac{\partial}{\partial z})^T$ and $\hat{\nabla} = (\frac{\partial}{\partial \hat{x}}, \frac{\partial}{\partial \hat{y}}, \frac{\partial}{\partial \hat{z}})^T$, respectively. Define the Laplace operator $\hat{\Delta}$ on $\hat{\Omega}$ by $\hat{\Delta} = \frac{\partial^2}{\partial \hat{x}^2} + \frac{\partial^2}{\partial \hat{y}^2} + \frac{\partial^2}{\partial \hat{z}^2}$.
By direct calculation, we have

$$A\nabla u = P^T \Lambda^{\frac{1}{2}} \nabla \hat{u} = S^{-1} \hat{\nabla} \hat{u}, \quad \text{and} \quad \nabla \cdot A\nabla u = \hat{\nabla} \cdot (\hat{\nabla} \hat{u}) \stackrel{\Delta}{=} \hat{\Delta} \hat{u}.$$

Thus, the anisotropic Helmholtz equation (2.1) is transformed into the isotropic Helmholtz equation

$$(2.13) \quad \hat{\Delta} \hat{u} + \omega^2 \hat{u} = 0 \quad \text{in} \quad \hat{\Omega}.$$

Conversely, if \hat{u} satisfies the isotropic Helmholtz equation (2.13), the function $u(\mathbf{x}) = \hat{u}(S\mathbf{x})$ satisfies the original anisotropic Helmholtz equation (2.1).

In order to define suitable anisotropic plane wave basis functions, we first define plane wave basis functions $\{y_{kl}\}$ satisfying the isotropic Helmholtz equation (2.13) on $\hat{\Omega}_k$ as follows.

$$(2.14) \quad \begin{cases} y_{kl}(\hat{\mathbf{x}}) = e^{i\omega(\hat{\mathbf{x}} \cdot \mathbf{d}_l)}, & \hat{\mathbf{x}} \in \hat{\Omega}_k, \\ \mathbf{d}_l \cdot \mathbf{d}_l = 1, \\ l \neq s \rightarrow \mathbf{d}_l \neq \mathbf{d}_s, \end{cases}$$

where \mathbf{d}_l ($l = 1, \dots, p$) are unit wave propagation directions, and can be determined by the codes in [22]. Choose the number p of plane wave propagation directions as $p = (m + 1)^2$, where m is a positive integer.

Then the anisotropic plane wave basis functions of $V_p(\mathcal{T}_h)$ can be defined as

$$(2.15) \quad u_{kl}(\mathbf{x}) = \begin{cases} y_{kl}(S\mathbf{x}), & \mathbf{x} \in \Omega_k, \\ 0, & \mathbf{x} \in \Omega_j \text{ satisfying } j \neq k \end{cases} \quad (k, j = 1, \dots, N; l = 1, \dots, p).$$

Thus the space $V(\mathcal{T}_h)$ is discretized by the subspace

$$(2.16) \quad V_p(\mathcal{T}_h) = \text{span}\{u_{kl} : k = 1, \dots, N; l = 1, \dots, p\}.$$

Furthermore, we obtain the discretized version of the continuous variational problem (2.8): Find $u_h \in V_p(\mathcal{T}_h)$ such that

$$(2.17) \quad \mathcal{A}_h(u_h, v_h) = \ell_h(v_h), \quad \forall v_h \in V_p(\mathcal{T}_h).$$

2.3. Error estimates of the approximate solutions. In this subsection, we are devoted to the analysis of convergence of the plane wave approximation u_h .

2.3.1. The required partition. In order to derive the desired error estimates of the approximate solutions, we require that the partition must satisfy some assumptions. In this part we introduce a kind of particular triangulation such that these assumptions can be met.

We adopt a non-regular triangulation \mathcal{T}_h for the three-dimensional **convex** domain Ω as follows (see Figure 1).

Mesh Generation Algorithm:

Step 1. Determine the image domain $\hat{\Omega}$ of Ω under the coordinate transformation (2.12).

Step 2. Decompose $\hat{\Omega}$ into polyhedron elements $\{\hat{\Omega}_k\}$ such that $\hat{\mathcal{T}}_h$ is shape regular and quasi-uniform in the usual manner. **Besides, we assume that each element $\hat{\Omega}_k$ of $\hat{\mathcal{T}}_h$ is a convex Lipschitz domain.**

Step 3. Determine the triangulation \mathcal{T}_h of Ω by using the inverse transformation of (2.12) acting on the elements of $\hat{\mathcal{T}}_h$.

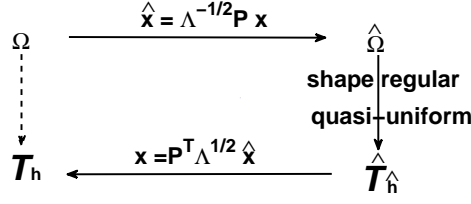


FIG. 1. Mesh generation.

REMARK 2.1. Notice that the coordinate transformation (2.12) consists of the orthogonal transformation P and the scaling transformation $\Lambda^{-\frac{1}{2}}$. It is known that an orthogonal matrix preserves the length of any vector and the angle between two vectors, then the orthogonal transformation preserves the shape of any polyhedron. Thus, it is cheap to determine the image domain $\hat{\Omega}$ and the triangulation \mathcal{T}_h by the coordinate transformation (2.12) and its inverse transformation, respectively, since we need only to compute the coordinates of the vertices of the polyhedron $\hat{\Omega}$ and the elements Ω_k .

For a 3×3 matrix B , we define

$$(2.18) \quad \|B\| = \|B\|_2 = \max_{\mathbf{0} \neq \mathbf{x} \in \mathbb{R}^3} \frac{\|B\mathbf{x}\|_2}{\|\mathbf{x}\|_2},$$

where $\mathbf{x} = (x_1, x_2, x_3)^T$ and $\|\mathbf{x}\|_2 = (x_1^2 + x_2^2 + x_3^2)^{\frac{1}{2}}$. Then it is well known that $\|A\| = \|A\| = \|\Lambda^{\frac{1}{2}}\|^2$. For the simplicity of notation, let ρ denote the condition number $\text{cond}(A)$ of the anisotropic matrix A . Then $\rho = \text{cond}(\Lambda) = \text{cond}^2(\Lambda^{\frac{1}{2}}) = \text{cond}^2(S)$.

The following Lemma gives an important geometric property of the triangulations.

LEMMA 2.2. For the proposed triangulation, we have

$$(2.19) \quad c_0 \|\Lambda^{\frac{1}{2}}\|^{-1} h \leq \hat{h} \leq C_0 \|\Lambda^{\frac{1}{2}}\|^{-1} h,$$

where c_0 and C_0 denote two constants independent of ω, ρ, h, p .

Proof. Let us first recall the definition of the shape regularity and quasi-uniformity assumptions. There exists a constant C independent of $\hat{\Omega}_k$ and $\hat{\mathcal{T}}_h$ such that for all $\hat{\Omega}_k \in \hat{\mathcal{T}}_h$ and all $\hat{\mathcal{T}}_h$,

$$(2.20) \quad \frac{\hat{h}_k}{\hat{\rho}_k} \leq C \quad \text{and} \quad \frac{\hat{h}}{\hat{h}_k} \leq C,$$

where \hat{h}_k denotes the diameter of the minimum sphere containing the polyhedron $\hat{\Omega}_k$, $\hat{\rho}_k$ denotes the diameter of the maximum sphere contained by the polyhedron $\hat{\Omega}_k$.

For convenience, we define two sub-transformation $\tilde{\mathbf{x}} = P\mathbf{x}$ and $\hat{\tilde{\mathbf{x}}} = \Lambda^{-\frac{1}{2}}\tilde{\mathbf{x}}$ to achieve the coordinate transformation (2.12). At first we consider the transformation

$$(2.21) \quad \hat{\tilde{\mathbf{x}}} = (\hat{x} \hat{y} \hat{z})^T = \Lambda^{-\frac{1}{2}} \tilde{\mathbf{x}} = (\tilde{x} \tilde{y} \tilde{z})^T.$$

For each element $\hat{\Omega}_k \in \hat{\mathcal{T}}_h$, we use $\hat{v}_k^{(i)}$ ($i = 1, 2, \dots$) to denote all the vertices of the polyhedron $\hat{\Omega}_k$, and assume that $\hat{\Omega}_k$ and $\hat{v}_k^{(i)}$ are transformed to $\tilde{\Omega}_k$ and $\tilde{v}_k^{(i)}$ under the inverse transformation of (2.21), respectively. We denote by \tilde{h}_k the diameter of the minimum sphere

containing the polyhedron $\tilde{\Omega}_k$, and by $\tilde{\rho}_k$ the diameter of the maximum sphere contained by the polyhedron $\tilde{\Omega}_k$, and set $\tilde{h} = \max_k \tilde{h}_k$.

Define $\Delta\hat{x}_k, \Delta\hat{y}_k$ and $\Delta\hat{z}_k$ as

$$(2.22) \quad \Delta\hat{x}_k = \max_{i,j} \left(\overrightarrow{\hat{v}_k^{(i)} \hat{v}_k^{(j)}} \right)_{\hat{x}}, \quad \Delta\hat{y}_k = \max_{i,j} \left(\overrightarrow{\hat{v}_k^{(i)} \hat{v}_k^{(j)}} \right)_{\hat{y}}, \quad \Delta\hat{z}_k = \max_{i,j} \left(\overrightarrow{\hat{v}_k^{(i)} \hat{v}_k^{(j)}} \right)_{\hat{z}}.$$

Here $\left(\overrightarrow{\hat{\mathbf{a}}} \right)_{\hat{x}} = a_1$, $\left(\overrightarrow{\hat{\mathbf{a}}} \right)_{\hat{y}} = a_2$ and $\left(\overrightarrow{\hat{\mathbf{a}}} \right)_{\hat{z}} = a_3$ for a vector $\overrightarrow{\hat{\mathbf{a}}} = (a_1 \ a_2 \ a_3)^T$. It follows by (2.20) that

$$(2.23) \quad c\hat{h}_k \leq \hat{\rho}_k \leq \Delta\hat{x}_k \leq \hat{h}_k, \quad c\hat{h}_k \leq \hat{\rho}_k \leq \Delta\hat{y}_k \leq \hat{h}_k, \quad c\hat{h}_k \leq \hat{\rho}_k \leq \Delta\hat{z}_k \leq \hat{h}_k$$

with $c = \frac{1}{C}$. Moreover, by the coordinate transformation (2.21), we have

$$(2.24) \quad \Delta\hat{x}_k = \frac{1}{\sqrt{\lambda_{\min}}} \Delta\tilde{x}_k, \quad \Delta\hat{y}_k = \frac{1}{\sqrt{\lambda_{\text{mid}}}} \Delta\tilde{y}_k, \quad \Delta\hat{z}_k = \frac{1}{\sqrt{\lambda_{\max}}} \Delta\tilde{z}_k,$$

where

$$(2.25) \quad \Delta\tilde{x}_k = \max_{i,j} \left(\overrightarrow{\tilde{v}_k^{(i)} \tilde{v}_k^{(j)}} \right)_{\tilde{x}}, \quad \Delta\tilde{y}_k = \max_{i,j} \left(\overrightarrow{\tilde{v}_k^{(i)} \tilde{v}_k^{(j)}} \right)_{\tilde{y}}, \quad \Delta\tilde{z}_k = \max_{i,j} \left(\overrightarrow{\tilde{v}_k^{(i)} \tilde{v}_k^{(j)}} \right)_{\tilde{z}}.$$

Combining (2.23) and (2.24), yields

$$(2.26) \quad c_1 \|\Lambda^{\frac{1}{2}}\| \hat{h}_k \leq \tilde{h}_k \leq C_1 \|\Lambda^{\frac{1}{2}}\| \hat{h}_k.$$

Then, by (2.20), we get

$$(2.27) \quad c_2 \|\Lambda^{\frac{1}{2}}\| \hat{h} \leq \tilde{h} \leq C_2 \|\Lambda^{\frac{1}{2}}\| \hat{h}.$$

Here c_i and C_i ($i = 1, 2$) denote different constants independent of ω, ρ, h, p and the triangulation \mathcal{T}_h .

Finally, since the orthogonal transformation $\tilde{\mathbf{x}} = P\mathbf{x}$ does not change the length of vectors and the angle between vectors, we obtain the desired result.

□

The next Lemma gives a relation between the areas of two bounded planes based on the coordinate transformation (2.12).

LEMMA 2.3. *For the proposed triangulation, denote by Γ a general bounded plane which belongs to \mathcal{F}_h , and by $\hat{\Gamma}$ the corresponding plane belonging to $\hat{\mathcal{F}}_h$. Then we have*

$$(2.28) \quad \frac{|\Gamma|}{|\hat{\Gamma}|} \leq \lambda_{\text{mid}}^{\frac{1}{2}} \lambda_{\max}^{\frac{1}{2}},$$

where $|f|$ denotes the area of a bounded plane f in the three-dimensional space.

Proof. In order to achieve the coordinate transformation (2.12), we also define two sub-transformation $\tilde{\mathbf{x}} = P\mathbf{x}$ and $\hat{\mathbf{x}} = \Lambda^{-\frac{1}{2}}\tilde{\mathbf{x}}$. Since the orthogonal transformation $\tilde{\mathbf{x}} = P\mathbf{x}$ does not change the length of vectors and the angle between vectors, we only need to prove the desired result under $\hat{\mathbf{x}} = (\hat{x} \ \hat{y} \ \hat{z})^T = \Lambda^{-\frac{1}{2}}\tilde{\mathbf{x}} = \Lambda^{-\frac{1}{2}}(\tilde{x} \ \tilde{y} \ \tilde{z})^T$, namely,

$$(2.29) \quad \tilde{\mathbf{x}} = \Lambda^{\frac{1}{2}}\hat{\mathbf{x}}.$$

Without loss of generality, consider $\Gamma : \tilde{z} = a\tilde{x} + b\tilde{y} + c$, $(\tilde{x}, \tilde{y}) \in D$, where a, b, c are constants, $D \subset \mathbb{R}^2$ is a bounded domain. By (2.29), we get $\hat{\Gamma} : \hat{z} = a(\frac{\lambda_{\min}}{\lambda_{\max}})^{\frac{1}{2}}\hat{x} + b(\frac{\lambda_{\min}}{\lambda_{\max}})^{\frac{1}{2}}\hat{y} + c(\frac{1}{\lambda_{\max}})^{\frac{1}{2}}$, $(\hat{x}, \hat{y}) \in \hat{D}$. Obviously, $\frac{|D|}{|\hat{D}|} = \det(\text{diag}(\lambda_{\min}^{\frac{1}{2}}, \lambda_{\min}^{\frac{1}{2}})) = \lambda_{\min}^{\frac{1}{2}} \lambda_{\min}^{\frac{1}{2}}$.

Thus,

$$(2.30) \quad |\Gamma| = \iint_D \sqrt{1 + \tilde{z}_x^2 + \tilde{z}_y^2} \, d\tilde{x}d\tilde{y} = \sqrt{1 + a^2 + b^2} |D|$$

and

$$(2.31) \quad |\hat{\Gamma}| = \iint_{\hat{D}} \sqrt{1 + \hat{z}_x^2 + \hat{z}_y^2} \, d\hat{x}d\hat{y} = \sqrt{1 + a^2 \frac{\lambda_{\min}}{\lambda_{\max}} + b^2 \frac{\lambda_{\min}}{\lambda_{\max}}} |\hat{D}|.$$

Combining the above equalities, we get

$$(2.32) \quad \frac{|\Gamma|}{|\hat{\Gamma}|} = \lambda_{\min}^{\frac{1}{2}} \lambda_{\min}^{\frac{1}{2}} \lambda_{\max}^{\frac{1}{2}} \frac{\sqrt{1 + a^2 + b^2}}{\sqrt{\lambda_{\max} + a^2 \lambda_{\min} + b^2 \lambda_{\min}}} \leq \lambda_{\min}^{\frac{1}{2}} \lambda_{\min}^{\frac{1}{2}} \lambda_{\max}^{\frac{1}{2}} \frac{\sqrt{1 + a^2 + b^2}}{\sqrt{\lambda_{\min} + a^2 \lambda_{\min} + b^2 \lambda_{\min}}} = \lambda_{\min}^{\frac{1}{2}} \lambda_{\max}^{\frac{1}{2}}.$$

□

2.3.2. Error analysis. Throughout this paper, we use C to denote a generic constant independent of A, ω, h, p, u and \hat{u} . The abstract error estimate built in [6] also holds in the current situation with the $\|\cdot\|_{\mathcal{F}_h}$ -norm.

LEMMA 2.4. *Let u be the analytical solution of (2.1)-(2.2), and let u_h be the approximate solution of (2.17). Then, we have*

$$(2.33) \quad \|u - u_h\|_{\mathcal{F}_h} \leq C \inf_{v_h \in V_p(\mathcal{T}_h)} \|u - v_h\|_{\mathcal{F}_h^+}.$$

For convenience, we use $\hat{V}(\hat{\mathcal{T}}_h)$ and $\hat{V}_p(\hat{\mathcal{T}}_h)$ to denote the images of $V(\mathcal{T}_h)$ and $V_p(\mathcal{T}_h)$ under the coordinate transformation (2.12), respectively. In addition, we define $\hat{u}_h(\hat{\mathbf{x}}) = u_h(S^{-1}\hat{\mathbf{x}})$, and endow the space $\hat{V}(\hat{\mathcal{T}}_h)$ with the norm

$$(2.34) \quad \begin{aligned} \|\hat{v}\|_{\hat{\mathcal{F}}_h}^2 &:= \omega^{-1} \|\beta^{1/2} \llbracket \hat{\mathbf{V}}_h \hat{v} \rrbracket_N\|_{0, \hat{\mathcal{F}}_h^I}^2 + \omega \|\alpha^{1/2} \llbracket \hat{v} \rrbracket_N\|_{0, \hat{\mathcal{F}}_h^I}^2 \\ &+ \omega^{-1} \|\delta^{1/2} \hat{\mathbf{V}}_h \hat{v} \cdot \hat{\mathbf{n}}\|_{0, \hat{\mathcal{F}}_h^B}^2 + \omega \|(1 - \delta)^{1/2} \hat{v}\|_{0, \hat{\mathcal{F}}_h^B}^2 \end{aligned}$$

and the augmented norm

$$(2.35) \quad \begin{aligned} \|\hat{v}\|_{\hat{\mathcal{F}}_h^+}^2 &:= \|\hat{v}\|_{\hat{\mathcal{F}}_h}^2 + \omega \|\beta^{-1/2} \{\{\hat{v}\}\}\|_{0, \hat{\mathcal{F}}_h^I}^2 \\ &+ \omega^{-1} \|\alpha^{-1/2} \{\{\hat{\mathbf{V}}_h \hat{v}\}\}\|_{0, \hat{\mathcal{F}}_h^I}^2 + \omega \|\delta^{-1/2} \hat{v}\|_{0, \hat{\mathcal{F}}_h^B}^2. \end{aligned}$$

The following Lemma states the transformation stability with respect to a mesh-dependent norm and a mesh-independent norm, respectively.

LEMMA 2.5. *For $u \in V(\mathcal{T}_h)$, we have*

$$(2.36) \quad \begin{aligned} \|u\|_{\mathcal{F}_h} &\leq \rho^{\frac{1}{2}} \lambda_{\min}^{\frac{1}{4}} \lambda_{\max}^{\frac{1}{4}} (1 + \lambda_{\min}^{\frac{1}{2}}) \|\hat{u}\|_{\hat{\mathcal{F}}_h}, \\ \|u\|_{\mathcal{F}_h^+} &\leq \rho^{\frac{1}{2}} \lambda_{\min}^{\frac{1}{4}} \lambda_{\max}^{\frac{1}{4}} (1 + \lambda_{\min}^{\frac{1}{2}}) \|\hat{u}\|_{\hat{\mathcal{F}}_h^+}, \end{aligned}$$

and

$$(2.37) \quad \|u\|_{0, \Omega} \leq \left(\det(\Lambda^{\frac{1}{2}}) \right)^{\frac{1}{2}} \|\hat{u}\|_{0, \hat{\Omega}}.$$

Proof. We divide the proof into three steps.

Step 1: To estimate $\|[[A\nabla_h u]]_N\|_{0,\mathcal{F}_h^I}$ and $\|A\nabla_h u \cdot \mathbf{n}\|_{0,\mathcal{F}_h^B}$.

By the coordinate transformation (2.12) and direct calculation, we obtain

$$(2.38) \quad \nabla u = P^T \Lambda^{-\frac{1}{2}} \hat{\nabla} \hat{u},$$

which implies that

$$(2.39) \quad A\nabla u = P^T \Lambda^{\frac{1}{2}} \hat{\nabla} \hat{u}.$$

Thus, on the interface $\Gamma_{kj} \in \mathcal{F}_h^I$, we have

$$(2.40) \quad [[A\nabla_h u]]_N = \mathbf{n}_k \cdot (P^T \Lambda^{\frac{1}{2}} \hat{\nabla}_{\hat{h}} \hat{u}_k) + \mathbf{n}_j \cdot (P^T \Lambda^{\frac{1}{2}} \hat{\nabla}_{\hat{h}} \hat{u}_j).$$

It is easy to check that

$$(2.41) \quad \mathbf{n}_k = |\Lambda^{\frac{1}{2}} P \mathbf{n}_k| P^T \Lambda^{-\frac{T}{2}} \hat{\mathbf{n}}_k.$$

Then

$$(2.42) \quad \mathbf{n}_k \cdot (P^T \Lambda^{\frac{1}{2}} \hat{\nabla}_{\hat{h}} \hat{u}_k) = |\Lambda^{\frac{1}{2}} P \mathbf{n}_k| \hat{\mathbf{n}}_k \cdot \hat{\nabla}_{\hat{h}} \hat{u}_k.$$

Substituting (2.42) into (2.40), yields

$$(2.43) \quad [[A\nabla_h u]]_N = |\Lambda^{\frac{1}{2}} P \mathbf{n}_k| [[\hat{\nabla}_{\hat{h}} \hat{u}]]_N.$$

Furthermore, by the scaling argument and **the relation (2.28)**, we obtain

$$(2.44) \quad \|[[A\nabla_h u]]_N\|_{0,\mathcal{F}_h^I} \leq \|\Lambda^{\frac{1}{2}}\| \lambda_{\text{mid}}^{\frac{1}{4}} \lambda_{\text{max}}^{\frac{1}{4}} \|[[\hat{\nabla}_{\hat{h}} \hat{u}]]_N\|_{0,\hat{\mathcal{F}}_h^I}$$

and

$$(2.45) \quad \|A\nabla_h u \cdot \mathbf{n}\|_{0,\mathcal{F}_h^B} \leq \|\Lambda^{\frac{1}{2}}\| \lambda_{\text{mid}}^{\frac{1}{4}} \lambda_{\text{max}}^{\frac{1}{4}} \|\hat{\nabla}_{\hat{h}} \hat{u}\|_{0,\hat{\mathcal{F}}_h^B}.$$

Step 2: To estimate $\|[[u]]_N\|_{0,\mathcal{F}_h^I}$.

By the coordinate transformation (2.12), we obtain

$$(2.46) \quad u_k \mathbf{n}_k = |\Lambda^{\frac{1}{2}} P \mathbf{n}_k| P^T \Lambda^{-\frac{T}{2}} (\hat{u}_k \hat{\mathbf{n}}_k).$$

Then, on the interface $\Gamma_{kj} \in \mathcal{F}_h^I$, we have

$$(2.47) \quad [[u]]_N = |\Lambda^{\frac{1}{2}} P \mathbf{n}_k| P^T \Lambda^{-\frac{T}{2}} [[\hat{u}]]_N.$$

Substituting (2.47) into $\|[[u]]_N\|_{0,\mathcal{F}_h^I}$ and combining with (2.28) and $|\Lambda^{\frac{1}{2}} P \mathbf{n}_k| \|P^T \Lambda^{-\frac{T}{2}}\| \leq \rho^{\frac{1}{2}}$, yields

$$(2.48) \quad \|[[u]]_N\|_{0,\mathcal{F}_h^I} \leq \rho^{\frac{1}{2}} \lambda_{\text{mid}}^{\frac{1}{4}} \lambda_{\text{max}}^{\frac{1}{4}} \|[[\hat{u}]]_N\|_{0,\hat{\mathcal{F}}_h^I}.$$

Step 3: Build estimates of $\|[\{u\}]\|_{0,\mathcal{F}_h^I}$, $\|[\{A\nabla_h u\}]\|_{0,\mathcal{F}_h^I}$ and $\|u\|_{0,\mathcal{F}_h^B}$.

By the coordinate transformation (2.12) and the scaling argument, we get

$$(2.49) \quad \|\{\{u\}\}\|_{0,\mathcal{F}_h^I} = \|\{\{\hat{u}\}\}\|_{0,\mathcal{F}_h^I} \leq \lambda_{\text{mid}}^{\frac{1}{4}} \lambda_{\text{max}}^{\frac{1}{4}} \|\{\{\hat{u}\}\}\|_{0,\hat{\mathcal{F}}_h^I},$$

$$(2.50) \quad \|\{\{A\nabla_h u\}\}\|_{0,\mathcal{F}_h^I} \stackrel{(2.39)}{=} \|P^T \Lambda^{\frac{1}{2}} \{\{\hat{\nabla}_h \hat{u}\}\}\|_{0,\mathcal{F}_h^I} \leq \|\Lambda^{\frac{1}{2}}\| \lambda_{\text{mid}}^{\frac{1}{4}} \lambda_{\text{max}}^{\frac{1}{4}} \|\{\{\hat{\nabla}_h \hat{u}\}\}\|_{0,\hat{\mathcal{F}}_h^I},$$

and

$$(2.51) \quad \|u\|_{0,\mathcal{F}_h^B} \leq \lambda_{\text{mid}}^{\frac{1}{4}} \lambda_{\text{max}}^{\frac{1}{4}} \|\hat{u}\|_{0,\hat{\mathcal{F}}_h^B}.$$

Combining (2.44)-(2.45) with (2.48)-(2.51) yields the desired result (2.36).

Finally, by the coordinate transformation (2.12) and the scaling argument, we directly obtain the result (2.37).

□

REMARK 2.2. *As in the proof of the above Lemma, we can obtain the following transformation stability with respect to two mesh-dependent norms, for $\forall \hat{u} \in \hat{V}(\hat{\mathcal{T}}_h)$,*

$$(2.52) \quad \begin{aligned} \|\hat{u}\|_{\hat{\mathcal{F}}_h} &\leq \rho^{\frac{1}{2}} \lambda_{\text{min}}^{-\frac{1}{4}} \lambda_{\text{mid}}^{-\frac{1}{4}} (1 + \lambda_{\text{max}}^{-\frac{1}{2}}) \|u\|_{\mathcal{F}_h}, \\ \|\hat{u}\|_{\hat{\mathcal{F}}_h^+} &\leq \rho^{\frac{1}{2}} \lambda_{\text{min}}^{-\frac{1}{4}} \lambda_{\text{mid}}^{-\frac{1}{4}} (1 + \lambda_{\text{max}}^{-\frac{1}{2}}) \|u\|_{\mathcal{F}_h^+}. \end{aligned}$$

Set $\hat{\lambda} = \min_{\hat{\Omega}_k \in \hat{\mathcal{T}}_h} \hat{\lambda}_k$, where $\hat{\lambda}_k$ is the positive parameter depending only on the shape of an element $\hat{\Omega}_k$ of $\hat{\mathcal{T}}_h$ introduced in [18, Theorem 3.2]. Let m be a given positive integer satisfying $m \geq 2(1 + 2^{1/\hat{\lambda}})$.

For a bounded and connected domain $D \subset \Omega$, let $\|\cdot\|_{s,\omega,D}$ be the ω -weighted Sobolev norm defined by

$$\|v\|_{s,\omega,D}^2 = \sum_{j=0}^s \omega^{2(s-j)} |v|_{j,D}^2.$$

The following Lemma is a direct consequence of Lemma 3.7 in [6] and Corollary 5.5 in [18].

LEMMA 2.6. *Let $1 < r \leq \frac{m-1}{2}$ with a sufficiently large m . Assume that the analytical solution $\hat{u} \in H^{r+1}(\hat{\Omega})$ satisfies the Helmholtz equation (2.13) in isotropic media. Then there is a function $\hat{\xi}_h \in \hat{V}_p(\hat{\mathcal{T}}_h)$ such that*

$$(2.53) \quad \|\hat{u} - \hat{\xi}_h\|_{\hat{\mathcal{F}}_h^+} \leq C_1 \omega^{-\frac{1}{2}} \hat{h}^{r-\frac{1}{2}} m^{-\lambda(r-\varepsilon)} \|\hat{u}\|_{r+1,\omega,\hat{\Omega}},$$

and

$$(2.54) \quad \|\hat{u}\|_{0,\hat{\Omega}} \leq C (\hat{h}^{1/2} \omega^{1/2} + \hat{h}^{-1/2} \omega^{-1/2}) \|\hat{u}\|_{\hat{\mathcal{F}}_h},$$

where $C_1 = C_1(\omega\hat{h})$ is independent of p and \hat{u} , but increases as a function of the product $\omega\hat{h}$ and depends on the shape of the $\hat{\Omega}_k \in \hat{\mathcal{T}}_h$, the index r and the flux parameters. $\varepsilon = \varepsilon(m) > 0$ satisfies $\varepsilon(m) \rightarrow 0$ when $m \rightarrow \infty$.

Based on the above discussions, we can easily build the desired error estimates of the approximation u_h .

THEOREM 2.7. *Let u and u_h denote the analytical solution of (2.1)-(2.2) and the proposed PWDG approximation, respectively. Suppose that p and r satisfy the conditions in Lemma 2.6. Assume that $\omega \hat{h} \leq C$ and $u \in H^{r+1}(\Omega)$. Then, for sufficiently large p , we have*

$$(2.55) \quad \left\| \|u - u_h\| \right\|_{\mathcal{F}_h^+} \leq C C_2 \rho^{\frac{3}{4}} \omega^{-\frac{1}{2}} h^{r-\frac{1}{2}} m^{-\hat{\lambda}(r-\varepsilon)} \|u\|_{r+1,\omega,\Omega},$$

and

$$(2.56) \quad \|u - u_h\|_{0,\Omega} \leq C C_3 \rho^{\frac{5}{4}} \omega^{-1} h^{r-1} m^{-\hat{\lambda}(r-\varepsilon)} \|u\|_{r+1,\omega,\Omega},$$

where the positive numbers C_2 and C_3 are defined as

$$C_2 = \|A^{\frac{1}{2}}\| (1 + \|A^{-\frac{1}{2}}\|^{-1}) \quad \text{and} \quad C_3 = (1 + \|A^{-\frac{1}{2}}\|^{-1}) (\|A\| + \|A^{\frac{1}{2}}\|).$$

Proof. With the transformations (2.12), we define $\xi_h(\mathbf{x}) = \hat{\xi}_h(S\mathbf{x})$, where $\hat{\xi}_h$ satisfying (2.53) denotes the plane wave approximation of the scaled acoustic field \hat{u} . **Under the assumption $\omega \hat{h} \leq C$, we have $C_1(\omega \hat{h}) \leq C$.** Thus, using (2.33) and (2.36), together with (2.53), leads to

$$(2.57) \quad \begin{aligned} \left\| \|u - u_h\| \right\|_{\mathcal{F}_h} &\leq C \left\| \|u - \xi_h\| \right\|_{\mathcal{F}_h^+} \leq C \rho^{\frac{1}{2}} \lambda_{\text{mid}}^{\frac{1}{4}} \lambda_{\text{max}}^{\frac{1}{4}} (1 + \lambda_{\text{min}}^{\frac{1}{2}}) \left\| \|\hat{u} - \hat{\xi}_h\| \right\|_{\hat{\mathcal{F}}_h^+} \\ &\leq C \rho^{\frac{1}{2}} \lambda_{\text{mid}}^{\frac{1}{4}} \lambda_{\text{max}}^{\frac{1}{4}} (1 + \lambda_{\text{min}}^{\frac{1}{2}}) \omega^{-\frac{1}{2}} \hat{h}^{r-\frac{1}{2}} m^{-\hat{\lambda}(r-\varepsilon)} \|\hat{u}\|_{r+1,\omega,\hat{\Omega}}. \end{aligned}$$

Then, by the scaling argument and (2.19), we further obtain

$$(2.58) \quad \begin{aligned} \left\| \|u - u_h\| \right\|_{\mathcal{F}_h} &\leq C \rho^{\frac{1}{2}} \omega^{-\frac{1}{2}} h^{r-\frac{1}{2}} m^{-\hat{\lambda}(r-\varepsilon)} \lambda_{\text{mid}}^{\frac{1}{4}} \lambda_{\text{max}}^{\frac{1}{4}} (1 + \lambda_{\text{min}}^{\frac{1}{2}}) \|\Lambda^{\frac{1}{2}}\|^{\frac{3}{2}} (\det(\Lambda^{-\frac{1}{2}}))^{\frac{1}{2}} \|u\|_{r+1,\omega,\Omega} \\ &\leq C \|\Lambda^{\frac{1}{2}}\| (1 + \|\Lambda^{-\frac{1}{2}}\|^{-1}) \rho^{\frac{3}{4}} \omega^{-\frac{1}{2}} h^{r-\frac{1}{2}} m^{-\hat{\lambda}(r-\varepsilon)} \|u\|_{r+1,\omega,\Omega}. \end{aligned}$$

Combining (2.37), (2.54), (2.19), (2.52) and (2.58), yields

$$\begin{aligned} \|u - u_h\|_{0,\Omega} &\stackrel{(2.37)}{\leq} \left(\det(\Lambda^{\frac{1}{2}}) \right)^{\frac{1}{2}} \|\hat{u} - \hat{u}_h\|_{0,\hat{\Omega}} \\ &\stackrel{(2.54)}{\leq} C \left(\det(\Lambda^{\frac{1}{2}}) \right)^{\frac{1}{2}} (\omega^{-\frac{1}{2}} \hat{h}^{-\frac{1}{2}} + \omega^{\frac{1}{2}} \hat{h}^{\frac{1}{2}}) \left\| \|\hat{u} - \hat{u}_h\| \right\|_{\hat{\mathcal{F}}_h} \\ &\stackrel{(2.19)}{\leq} C \left(\det(\Lambda^{\frac{1}{2}}) \right)^{\frac{1}{2}} \omega^{-\frac{1}{2}} h^{-\frac{1}{2}} \|\Lambda^{\frac{1}{2}}\|^{\frac{1}{2}} \left\| \|\hat{u} - \hat{u}_h\| \right\|_{\hat{\mathcal{F}}_h} \\ &\stackrel{(2.52)}{\leq} C \left(\det(\Lambda^{\frac{1}{2}}) \right)^{\frac{1}{2}} \omega^{-\frac{1}{2}} h^{-\frac{1}{2}} \|\Lambda^{\frac{1}{2}}\|^{\frac{1}{2}} \rho^{\frac{1}{2}} \lambda_{\text{min}}^{-\frac{1}{4}} \lambda_{\text{mid}}^{-\frac{1}{4}} (1 + \lambda_{\text{max}}^{-\frac{1}{2}}) \left\| \|u - u_h\| \right\|_{\mathcal{F}_h} \\ &\stackrel{(2.58)}{\leq} C C_3 \rho^{\frac{5}{4}} \omega^{-1} h^{r-1} m^{-\hat{\lambda}(r-\varepsilon)} \|u\|_{r+1,\omega,\Omega}, \end{aligned}$$

This completes the proof. \square

REMARK 2.3. *We emphasize that **the shape regularity assumption** on the triangulation $\hat{\mathcal{T}}_h$ (instead of \mathcal{T}_h) is important in the derivation of the error estimate (2.56). In fact, if we directly assume that the triangulation \mathcal{T}_h is shape regular, we have different relations on the two mesh sizes:*

$$(2.59) \quad \|\Lambda^{\frac{1}{2}}\|^{-1} h \leq \hat{h} \leq \|\Lambda^{-\frac{1}{2}}\| h.$$

In this situation, we can only build a weaker L^2 error estimate than (2.56)

$$(2.60) \quad \|u - u_h\|_{0,\Omega} \leq C C_3 \rho^{\frac{r}{2}+1} \omega^{-1} h^{r-1} m^{-\theta \hat{\lambda}(r-\varepsilon)} \|u\|_{r+1,\omega,\Omega} \quad (r > 1)$$

REMARK 2.4. A natural idea is to apply the standard PWDG method to the isotropic Helmholtz equation (2.13) derived by the transformation S and then use the image of the resulting approximation under the inverse transformation S^{-1} as the desired approximation of u , but this idea may be disappointing. Let $\hat{u}(\hat{\mathbf{x}})$ and $\tilde{u}_h(\hat{\mathbf{x}})$ denote the analytic solution of the equation (2.13) and its PWDG approximation, respectively, and let $\tilde{u}_h(\mathbf{x})$ denote the image of $\tilde{u}_h(\hat{\mathbf{x}})$ under the inverse transformation S^{-1} . Although the following abstract error estimate is still valid

$$(2.61) \quad \|\hat{u} - \tilde{u}_h\|_{\hat{\mathcal{F}}_h} \leq \inf_{\hat{\xi}_h \in \hat{V}_p(\hat{\mathcal{T}}_h)} \|\hat{u} - \hat{\xi}_h\|_{\hat{\mathcal{F}}_h^+},$$

the approximation \tilde{u}_h does not satisfy the abstract error estimate (2.33). Then it seems impossible to build a desired error estimate of the approximation \tilde{u}_h . In fact, by (2.43) and (2.47), we have

$$\llbracket A \nabla_h v \rrbracket_N = |\Lambda^{\frac{1}{2}} P \mathbf{n}_k| \llbracket \hat{\nabla}_h \hat{v} \rrbracket_N \quad \text{and} \quad \llbracket v \rrbracket_N = |\Lambda^{\frac{1}{2}} P \mathbf{n}_k| P^T \Lambda^{\frac{-T}{2}} \llbracket \hat{v} \rrbracket_N \quad \text{on } \Gamma_{kj} \in \mathcal{F}_h^I.$$

The different factors in the right hands of these relations tell us that the proposed PWDG approximation u_h is indeed different from the image $\tilde{u}_h(\mathbf{x})$ of $\tilde{u}_h(\hat{\mathbf{x}})$ under the inverse transformation S^{-1} .

3. Plane wave method for three-dimensional anisotropic time-harmonic Maxwell's equations. In this section we extend the method proposed in the last section to time-harmonic Maxwell's equations in three-dimensional anisotropic media. As we will see, the current situation is more complex than the case of Helmholtz equation.

3.1. The model and its variational formula. We consider three-dimensional time-harmonic Maxwell equations written as a first-order system of equations:

$$(3.1) \quad \begin{cases} \nabla \times \mathbf{E} - i\omega\mu\mathbf{H} = \mathbf{0} \\ \nabla \times \mathbf{H} + i\omega\varepsilon\mathbf{E} = \mathbf{0} \\ \nabla \cdot (\varepsilon\mathbf{E}) = 0 \\ \nabla \cdot (\mu\mathbf{H}) = 0 \end{cases} \quad \text{in } \Omega$$

with the lowest-order absorbing boundary condition

$$(3.2) \quad \mathbf{H} \times \mathbf{n} - \vartheta(\mathbf{n} \times \mathbf{E}) \times \mathbf{n} = \mathbf{g}/i\omega \quad \text{on } \gamma = \partial\Omega.$$

Here $\mathbf{E} = (E_x, E_y, E_z)^T$, $\mathbf{H} = (H_x, H_y, H_z)^T$; $\omega > 0$ is the temporal frequency of the field; $\vartheta \neq 0$ is assumed to be constant; $\mathbf{g} \in L^2(\partial\Omega)$. The permittivity ε and the permeability μ are assumed to be of the form

$$(3.3) \quad \begin{aligned} \varepsilon &= \varepsilon_r A, \\ \mu &= \mu_r A. \end{aligned}$$

where ε_r, μ_r are constant, and A is assumed to be real strictly positive definite matrix.

We also denote by \mathcal{T}_h the partition of the domain Ω , which is also a bounded polyhedron. Define the broken Sobolev space

$$(3.4) \quad \mathbf{H}^r(\text{curl}; \mathcal{T}_h) = \{\mathbf{w} \in L^2(\Omega)^3 : \mathbf{w}|_{\Omega_k} \in \mathbf{H}^r(\text{curl}; \Omega_k) \quad \forall \Omega_k \in \mathcal{T}_h\}.$$

Let $\mathbf{V}(\mathcal{T}_h)$ be the piecewise Trefftz space defined on \mathcal{T}_h by

$$(3.5) \quad \mathbf{V}(\mathcal{T}_h) = \left\{ \mathbf{w} \in L^2(\Omega)^3 : \exists s > 0 \text{ s.t. } \mathbf{w} \in \mathbf{H}^{1/2+s}(\text{curl}; \mathcal{T}_h), \right. \\ \left. \text{and } \nabla \times (\mu^{-1} \nabla \times \mathbf{w}) - \omega^2 \varepsilon \mathbf{w} = \mathbf{0} \text{ in each } \Omega_k \in \mathcal{T}_h \right\}.$$

Let α, β, δ be strictly positive constants, with $0 < \delta \leq 1/2$. Define the sesquilinear form $\mathcal{A}_h(\cdot, \cdot)$ by

$$\begin{aligned} \mathcal{A}_h(\mathbf{E}, \boldsymbol{\xi}) = & - \int_{\mathcal{F}_h^1} \{ \{\mathbf{E}\} \} \cdot \overline{\llbracket \mu^{-1} \nabla_h \times \boldsymbol{\xi} \rrbracket_T} dS - i\omega^{-1} \int_{\mathcal{F}_h^1} \beta \llbracket \mu^{-1} \nabla_h \times \mathbf{E} \rrbracket_T \cdot \overline{\llbracket \mu^{-1} \nabla_h \times \boldsymbol{\xi} \rrbracket_T} dS \\ & - \int_{\mathcal{F}_h^1} \{ \{ \mu^{-1} \nabla_h \times \mathbf{E} \} \} \cdot \overline{\llbracket \boldsymbol{\xi} \rrbracket_T} dS - i\omega \int_{\mathcal{F}_h^1} \alpha \llbracket \mathbf{E} \rrbracket_T \cdot \overline{\llbracket \boldsymbol{\xi} \rrbracket_T} dS \\ & + \int_{\mathcal{F}_h^B} (1 - \delta) (\mathbf{n} \times \mathbf{E}) \cdot \overline{(\mu^{-1} \nabla_h \times \boldsymbol{\xi})} dS - \int_{\mathcal{F}_h^B} \delta (\mu^{-1} \nabla_h \times \mathbf{E}) \cdot \overline{(\mathbf{n} \times \boldsymbol{\xi})} dS \\ & - i\omega^{-1} \int_{\mathcal{F}_h^B} \delta \vartheta^{-1} [\mathbf{n} \times (\mu^{-1} \nabla_h \times \mathbf{E})] \cdot \overline{[\mathbf{n} \times (\mu^{-1} \nabla_h \times \boldsymbol{\xi})]} dS \\ & - i\omega \int_{\mathcal{F}_h^B} (1 - \delta) \vartheta (\mathbf{n} \times \mathbf{E}) \cdot \overline{(\mathbf{n} \times \boldsymbol{\xi})} dS, \quad \forall \boldsymbol{\xi} \in \mathbf{V}(\mathcal{T}_h) \end{aligned}$$

and the functional $\ell_h(\cdot, \cdot)$ by

$$(3.6) \quad \ell_h(\mathbf{g}, \boldsymbol{\xi}) = -i\omega^{-1} \int_{\mathcal{F}_h^B} \delta \vartheta^{-1} (\mathbf{n} \times \mathbf{g}) \cdot \overline{\mu^{-1} \nabla_h \times \boldsymbol{\xi}} dS + \int_{\mathcal{F}_h^B} (1 - \delta) (\mathbf{n} \times \mathbf{g}) \cdot \overline{(\mathbf{n} \times \boldsymbol{\xi})} dS, \quad \forall \boldsymbol{\xi} \in \mathbf{V}(\mathcal{T}_h)$$

Then, for a given \mathbf{g} , the variational problem associated with (3.1)-(3.2) can be expressed as follows (see [9, Section 3]). Find $\mathbf{E} \in \mathbf{V}(\mathcal{T}_h)$ such that,

$$(3.7) \quad \mathcal{A}_h(\mathbf{E}, \boldsymbol{\xi}) = \ell_h(\mathbf{g}, \boldsymbol{\xi}), \quad \forall \boldsymbol{\xi} \in \mathbf{V}(\mathcal{T}_h).$$

3.2. Plane wave discretization for the 3D anisotropic Maxwell equations. The proposed plane wave method for (3.1) depends on two transformations.

3.2.1. A scaled transformation and a coordinate transformation. Since A is positive definite matrix, there exists an orthogonal matrix P and a diagonal positive definite matrix $\Lambda = \text{diag}(\lambda_{\min}, \lambda_{\text{mid}}, \lambda_{\max})$ such that $A = P^T \Lambda P$, where $\lambda_{\min} \leq \lambda_{\text{mid}} \leq \lambda_{\max}$ are constant. Without loss of generality, we also assume that $\det(P) = 1$. Furthermore, we set

$$(3.8) \quad m_{\max} = \sqrt{\lambda_{\text{mid}} \lambda_{\max}}, \quad m_{\text{mid}} = \sqrt{\lambda_{\max} \lambda_{\min}} \quad \text{and} \quad m_{\min} = \sqrt{\lambda_{\min} \lambda_{\text{mid}}}.$$

Define the scaled fields $\tilde{\mathbf{E}}$ and $\tilde{\mathbf{H}}$ as

$$(3.9) \quad \begin{aligned} (E_x, E_y, E_z)^T &= G (\tilde{E}_x, \tilde{E}_y, \tilde{E}_z)^T, \\ (H_x, H_y, H_z)^T &= G (\tilde{H}_x, \tilde{H}_y, \tilde{H}_z)^T. \end{aligned}$$

Here $G = P^T \Lambda^{-\frac{1}{2}}$. Then, by direct calculation on (3.9), we deduce that

$$\nabla \times \mathbf{E} = P^T \Lambda^{\frac{1}{2}} \left(-\frac{q_3 \cdot \nabla \tilde{E}_y}{m_{\min}} + \frac{q_2 \cdot \nabla \tilde{E}_z}{m_{\text{mid}}}, \frac{q_3 \cdot \nabla \tilde{E}_x}{m_{\min}} - \frac{q_1 \cdot \nabla \tilde{E}_z}{m_{\max}}, -\frac{q_2 \cdot \nabla \tilde{E}_x}{m_{\text{mid}}} + \frac{q_1 \cdot \nabla \tilde{E}_y}{m_{\max}} \right)^T,$$

$$\begin{aligned}
\nabla \times \mathbf{H} &= P^T \Lambda^{\frac{1}{2}} \left(-\frac{q_3 \cdot \nabla \tilde{H}_y}{m_{\min}} + \frac{q_2 \cdot \nabla \tilde{H}_z}{m_{\text{mid}}}, \frac{q_3 \cdot \nabla \tilde{H}_x}{m_{\min}} - \frac{q_1 \cdot \nabla \tilde{H}_z}{m_{\max}}, -\frac{q_2 \cdot \nabla \tilde{H}_x}{m_{\text{mid}}} + \frac{q_1 \cdot \nabla \tilde{H}_y}{m_{\max}} \right)^T, \\
\mu \mathbf{H} &= \mu_r P^T \Lambda P P^T \Lambda^{-\frac{1}{2}} \tilde{\mathbf{H}} = \mu_r P^T \Lambda^{\frac{1}{2}} \tilde{\mathbf{H}}, \\
\varepsilon \mathbf{E} &= \varepsilon_r P^T \Lambda P P^T \Lambda^{-\frac{1}{2}} \tilde{\mathbf{E}} = \varepsilon_r P^T \Lambda^{\frac{1}{2}} \tilde{\mathbf{E}}.
\end{aligned}
\tag{3.10}$$

Here we need to first use (3.3) for the derivation of the later two equalities.

Set $M = \text{diag}(m_{\max}, m_{\text{mid}}, m_{\min})$, and define the coordinate transformation

$$\hat{\mathbf{x}} = (\hat{x} \hat{y} \hat{z})^T = M P (x y z)^T \stackrel{\Delta}{=} S \mathbf{x}, \quad S = M P.
\tag{3.11}$$

With the inverse transformation S^{-1} , we define the scaled electric and magnetic fields

$$(\hat{\mathbf{E}}(\hat{\mathbf{x}}), \hat{\mathbf{H}}(\hat{\mathbf{x}}))^T = (\tilde{\mathbf{E}}(S^{-1}\hat{\mathbf{x}}), \tilde{\mathbf{H}}(S^{-1}\hat{\mathbf{x}}))^T = (\tilde{\mathbf{E}}(\mathbf{x}), \tilde{\mathbf{H}}(\mathbf{x}))^T.
\tag{3.12}$$

By direct manipulation on (3.12), we obtain the following system

$$\begin{aligned}
\hat{\nabla} \times \hat{\mathbf{E}} &= \left(-\frac{q_3 \cdot \nabla \tilde{E}_y}{m_{\min}} + \frac{q_2 \cdot \nabla \tilde{E}_z}{m_{\text{mid}}}, \frac{q_3 \cdot \nabla \tilde{E}_x}{m_{\min}} - \frac{q_1 \cdot \nabla \tilde{E}_z}{m_{\max}}, -\frac{q_2 \cdot \nabla \tilde{E}_x}{m_{\text{mid}}} + \frac{q_1 \cdot \nabla \tilde{E}_y}{m_{\max}} \right)^T, \\
\hat{\nabla} \times \hat{\mathbf{H}} &= \left(-\frac{q_3 \cdot \nabla \tilde{H}_y}{m_{\min}} + \frac{q_2 \cdot \nabla \tilde{H}_z}{m_{\text{mid}}}, \frac{q_3 \cdot \nabla \tilde{H}_x}{m_{\min}} - \frac{q_1 \cdot \nabla \tilde{H}_z}{m_{\max}}, -\frac{q_2 \cdot \nabla \tilde{H}_x}{m_{\text{mid}}} + \frac{q_1 \cdot \nabla \tilde{H}_y}{m_{\max}} \right)^T, \\
M \Lambda^{\frac{1}{2}} \hat{\nabla} \cdot \hat{\mathbf{H}} &= \nabla \cdot (P^T \Lambda^{\frac{1}{2}} \tilde{\mathbf{H}}), \\
M \Lambda^{\frac{1}{2}} \hat{\nabla} \cdot \hat{\mathbf{E}} &= \nabla \cdot (P^T \Lambda^{\frac{1}{2}} \tilde{\mathbf{E}}).
\end{aligned}
\tag{3.13}$$

Thus, by (3.1), (3.10) and (3.13), the scaled electric and magnetic fields $(\hat{\mathbf{E}}(\hat{\mathbf{x}}), \hat{\mathbf{H}}(\hat{\mathbf{x}}))$ satisfy the transformed isotropic Maxwell equations:

$$\begin{cases} \hat{\nabla} \times \hat{\mathbf{E}} - i\omega \mu_r \hat{\mathbf{H}} = \mathbf{0} \\ \hat{\nabla} \times \hat{\mathbf{H}} + i\omega \varepsilon_r \hat{\mathbf{E}} = \mathbf{0} \\ \hat{\nabla} \cdot (\varepsilon_r \hat{\mathbf{E}}) = 0 \\ \hat{\nabla} \cdot (\mu_r \hat{\mathbf{H}}) = 0 \end{cases} \quad \text{in } \hat{\Omega}.
\tag{3.14}$$

Conversely, if the scaled electric and magnetic fields $(\hat{\mathbf{E}}(\hat{\mathbf{x}}), \hat{\mathbf{H}}(\hat{\mathbf{x}}))$ satisfy the transformed isotropic Maxwell equations (3.14), the physical electromagnetic fields $(\mathbf{E}(\mathbf{x}), \mathbf{H}(\mathbf{x}))$

$$\begin{cases} \mathbf{E}(\mathbf{x}) = G \hat{\mathbf{E}}(\hat{\mathbf{x}}) = G \hat{\mathbf{E}}(S \mathbf{x}) \\ \mathbf{H}(\mathbf{x}) = G \hat{\mathbf{H}}(\hat{\mathbf{x}}) = G \hat{\mathbf{H}}(S \mathbf{x}) \end{cases}
\tag{3.15}$$

satisfy the original anisotropic Maxwell equations (3.1).

As in Section 2, let $\hat{\Omega}$ and $\hat{\Omega}_k$ denote the images of Ω and Ω_k under the coordinate transformation (3.11), respectively. In addition, let $\hat{\mathcal{T}}_{\hat{h}}$ denote the partition comprised of the elements $\{\hat{\Omega}_k\}$, where \hat{h} is the mesh size of the partition $\hat{\mathcal{T}}_{\hat{h}}$. Set $\hat{\mathcal{F}}_{\hat{h}} = \bigcup_k \partial \hat{\Omega}_k$, $\hat{\mathcal{F}}_{\hat{h}}^{\text{B}} = \partial \hat{\Omega}$ and $\hat{\mathcal{F}}_{\hat{h}}^{\text{I}} = \hat{\mathcal{F}}_{\hat{h}} \setminus \hat{\mathcal{F}}_{\hat{h}}^{\text{B}}$.

In the next subsection we present a plane wave discretization method for the considered anisotropic Maxwell equations by using the scaling matrix (3.9) and the coordinate transformation (3.11).

3.2.2. Anisotropic plane wave basis function spaces. The discretization is based on a finite-dimensional subspace $\mathbf{V}_p(\mathcal{T}_h) \subset \mathbf{V}(\mathcal{T}_h)$. We first define plane wave basis function space $\hat{\mathbf{V}}_p(\hat{\mathcal{T}}_{\hat{h}})$ satisfying the isotropic Maxwell equations (3.14).

By choosing p unit propagation directions \mathbf{d}_l ($l = 1, \dots, p$), which can be determined by the codes in [22], we can define plane wave functions $\hat{\mathbf{E}}_l$:

$$(3.16) \quad \hat{\mathbf{E}}_l = \mathbf{F}_l \exp(i \kappa \mathbf{d}_l \cdot \hat{\mathbf{x}}) \quad \text{and} \quad \hat{\mathbf{E}}_{l+p} = \mathbf{G}_l \exp(i \kappa \mathbf{d}_l \cdot \hat{\mathbf{x}}) \quad (l = 1, \dots, p),$$

where $\kappa = \omega \sqrt{\mu_r \varepsilon_r}$, \mathbf{F}_l and \mathbf{G}_l are polarization vectors satisfying $\mathbf{F}_l \cdot \mathbf{d}_l = 0$ and $\mathbf{G}_l = \mathbf{F}_l \times \mathbf{d}_l$ ($l = 1, \dots, p$).

Let $\hat{\mathcal{Q}}_{2p}$ denote the space spanned by the $2p$ plane wave functions $\hat{\mathbf{E}}_l$ ($l = 1, \dots, 2p$), and define the isotropic plane wave space

$$(3.17) \quad \hat{\mathbf{V}}_p(\hat{\mathcal{T}}_h) = \left\{ \hat{\mathbf{v}} \in L^2(\hat{\Omega}) : \hat{\mathbf{v}}|_{\hat{K}} \in \hat{\mathcal{Q}}_{2p} \text{ for any } \hat{K} \in \hat{\mathcal{T}}_h \right\}.$$

By (3.15), we can define the anisotropic plane wave basis functions satisfying the original equations (3.1):

$$(3.18) \quad \mathbf{E}_l = G \mathbf{F}_l \exp(i \kappa \mathbf{d}_l \cdot S \mathbf{x}) \quad \text{and} \quad \mathbf{E}_{l+p} = G \mathbf{G}_l \exp(i \kappa \mathbf{d}_l \cdot S \mathbf{x}) \quad (l = 1, \dots, p).$$

Let \mathcal{Q}_{2p} denote the space spanned by the $2p$ plane wave basis functions \mathbf{E}_l ($l = 1, \dots, 2p$), and define the anisotropic plane wave space

$$(3.19) \quad \mathbf{V}_p(\mathcal{T}_h) = \left\{ \mathbf{v} \in L^2(\Omega) : \mathbf{v}|_K \in \mathcal{Q}_{2p} \text{ for any } K \in \mathcal{T}_h \right\}.$$

It is clear that the above space has $N \times 2p$ basis functions, which are defined by

$$(3.20) \quad \phi_l^k(\mathbf{x}) = \begin{cases} \mathbf{E}_l(\mathbf{x}), & \mathbf{x} \in \Omega_k, \\ 0, & \mathbf{x} \in \Omega_j \text{ satisfying } j \neq k \end{cases} \quad (k = 1, \dots, N; l = 1, \dots, 2p).$$

Furthermore, for a given \mathbf{g} , we obtain the discretized version of the continuous variational problem (3.7): Find $\mathbf{E}_h \in \mathbf{V}_p(\mathcal{T}_h)$ such that,

$$(3.21) \quad \mathcal{A}_h(\mathbf{E}_h, \boldsymbol{\xi}_h) = \ell_h(\mathbf{g}, \boldsymbol{\xi}_h), \quad \forall \boldsymbol{\xi}_h \in \mathbf{V}_p(\mathcal{T}_h).$$

For convenience, we use $\hat{\mathbf{V}}(\hat{\mathcal{T}}_h)$ to denote the image space of the space $\mathbf{V}(\mathcal{T}_h)$ under the scaling transformation (3.9) and the coordinate transformation (3.11), and set $\hat{\mathbf{E}}_h(\hat{\mathbf{x}}) = G^{-1} \mathbf{E}_h(S^{-1} \hat{\mathbf{x}})$.

3.3. Error estimates of the approximate solutions. For the simplicity of notation, we also use ρ to denote the condition number $\text{cond}(A)$ for the positive definite matrix A defined in (3.3). It is easy to see that $\text{cond}(A) = \text{cond}(\Lambda)$ and $\text{cond}(S) = \text{cond}(M) = \rho^{\frac{1}{2}}$.

We adopt similar steps described in section 2 to partition Ω . The minor difference is that, under the coordinate transformation (3.11), we have

$$(3.22) \quad c_0 \|M^{-1}\|^{-1} h \leq \hat{h} \leq C_0 \|M^{-1}\|^{-1} h.$$

We endow $\mathbf{V}(\mathcal{T}_h)$ with the mesh-skeleton norm,

$$(3.23) \quad \begin{aligned} \|\mathbf{w}\|_{\mathcal{F}_h}^2 &= \omega^{-1} \|\beta^{1/2} \llbracket \mu^{-1} \nabla_h \times \mathbf{w} \rrbracket_T\|_{0, \mathcal{F}_h^I}^2 + \omega \|\alpha^{1/2} \llbracket \mathbf{w} \rrbracket_T\|_{0, \mathcal{F}_h^I}^2 \\ &\quad + \omega^{-1} \|\delta^{1/2} \vartheta^{-1/2} \mathbf{n} \times (\mu^{-1} \nabla_h \times \mathbf{w})\|_{0, \mathcal{F}_h^B}^2 + \omega \|(1 - \delta)^{1/2} \vartheta^{1/2} \mathbf{n} \times \mathbf{w}\|_{0, \mathcal{F}_h^B}^2 \end{aligned}$$

and the following augmented norm

$$(3.24) \quad \begin{aligned} \|\mathbf{w}\|_{\mathcal{F}_h^+}^2 &= \|\mathbf{w}\|_{\mathcal{F}_h}^2 + \omega \|\beta^{-1/2} \{\{\mathbf{w}\}\}\|_{0, \mathcal{F}_h^I}^2 \\ &\quad + \omega^{-1} \|\alpha^{-1/2} \{\{\mu^{-1} \nabla_h \times \mathbf{w}\}\}\|_{0, \mathcal{F}_h^I}^2 + \omega \|\delta^{-1/2} \vartheta^{1/2} (\mathbf{n} \times \mathbf{w})\|_{0, \mathcal{F}_h^B}^2. \end{aligned}$$

Similarly, we endow $\hat{\mathbf{V}}(\hat{\mathcal{T}}_h)$ with the mesh-skeleton norm, which were introduced in [9],

$$(3.25) \quad \begin{aligned} \|\hat{\mathbf{w}}\|_{\hat{\mathcal{T}}_h}^2 &= \omega^{-1} \|\beta^{1/2} \llbracket \mu_r^{-1} \hat{\mathbf{v}}_h \times \hat{\mathbf{w}} \rrbracket_T\|_{0, \hat{\mathcal{T}}_h^I}^2 + \omega \|\alpha^{1/2} \llbracket \hat{\mathbf{w}} \rrbracket_T\|_{0, \hat{\mathcal{T}}_h^I}^2 \\ &\quad + \omega^{-1} \|\delta^{1/2} \vartheta^{-1/2} \hat{\mathbf{n}} \times (\mu_r^{-1} \hat{\mathbf{v}}_h \times \hat{\mathbf{w}})\|_{0, \hat{\mathcal{T}}_h^B}^2 + \omega \|(1-\delta)^{1/2} \vartheta^{1/2} \hat{\mathbf{n}} \times \hat{\mathbf{w}}\|_{0, \hat{\mathcal{T}}_h^B}^2 \end{aligned}$$

and the following augmented norm

$$(3.26) \quad \begin{aligned} \|\hat{\mathbf{w}}\|_{\hat{\mathcal{T}}_h^+}^2 &= \|\hat{\mathbf{w}}\|_{\hat{\mathcal{T}}_h}^2 + \omega \|\beta^{-1/2} \{\{\hat{\mathbf{w}}\}\}\|_{0, \hat{\mathcal{T}}_h^I}^2 \\ &\quad + \omega^{-1} \|\alpha^{-1/2} \{\{\mu_r^{-1} \hat{\mathbf{v}}_h \times \hat{\mathbf{w}}\}\}\|_{0, \hat{\mathcal{T}}_h^I}^2 + \omega \|\delta^{-1/2} \vartheta^{1/2} (\hat{\mathbf{n}} \times \hat{\mathbf{w}})\|_{0, \hat{\mathcal{T}}_h^B}^2. \end{aligned}$$

As in [9], we can show the following existence, uniqueness and continuity results of solution of the above variational problem.

LEMMA 3.1. *There exists a unique solution \mathbf{E}_h of (3.7). Moreover, we have*

$$(3.27) \quad \begin{aligned} -\text{Im}[\mathcal{A}_h(\mathbf{w}, \mathbf{w})] &= \|\mathbf{w}\|_{\mathcal{F}_h}^2, \\ \text{and } |\mathcal{A}_h(\mathbf{w}, \boldsymbol{\xi})| &\leq 2 \|\mathbf{w}\|_{\mathcal{F}_h^+} \|\boldsymbol{\xi}\|_{\mathcal{F}_h}, \quad \forall \mathbf{w}, \boldsymbol{\xi} \in \mathbf{V}(\mathcal{T}_h). \end{aligned}$$

The abstract error estimate built in [9] also holds in the current situation with the

$\|\cdot\|_{\mathcal{F}_h}$ -norm.

LEMMA 3.2. *Let \mathbf{E} be the analytical solution of (3.1)-(3.2) and let \mathbf{E}_h be the approximate solution of (3.21). Then, there exists a constant C independent of ω, h, p and A such that*

$$(3.28) \quad \|\mathbf{E} - \mathbf{E}_h\|_{\mathcal{F}_h} \leq 3 \inf_{\boldsymbol{\xi}_h \in \mathbf{V}_p(\mathcal{T}_h)} \|\mathbf{E} - \boldsymbol{\xi}_h\|_{\mathcal{F}_h^+}.$$

Let m be a positive integer satisfying the condition described in Subsection 2.3.2, assume that $1 < r \leq \frac{m-1}{2}$ and choose $p = (m+1)^2$. The following Lemma is a direct consequence of Corollary 5.5 in [9].

LEMMA 3.3. *Assume that the analytical solution $\hat{\mathbf{E}} \in \mathbf{H}^{r+1}(\text{curl}; \hat{\Omega})$ satisfies the Maxwell equations (3.14) in isotropic media. Choose a set of p plane wave propagation directions $\{\mathbf{d}_l\}_{1 \leq l \leq p}$ with the corresponding set of polarization directions $\mathbf{F}_l, \mathbf{G}_l$ defined by (3.16) in a suitable manner. Then, there is a function $\hat{\boldsymbol{\xi}}_h \in \hat{\mathbf{V}}_p(\hat{\mathcal{T}}_h)$ such that, for large p ,*

$$(3.29) \quad \|\hat{\mathbf{E}} - \hat{\boldsymbol{\xi}}_h\|_{\hat{\mathcal{T}}_h^+} \leq C_1 \omega^{-5/2} \left(\frac{\hat{h}}{m^\lambda}\right)^{r-\frac{3}{2}} \|\hat{\mathbf{v}} \times \hat{\mathbf{E}}\|_{r+1, \omega, \hat{\Omega}},$$

where $C_1 = C_1(\omega \hat{h}) > 0$ is independent of p and $\hat{\mathbf{E}}$, but increases as a function of the product $\omega \hat{h}$, and C_1 depends on the shape of the $\hat{\Omega}_k \in \hat{\mathcal{T}}_h$, the index r , the material parameters $\vartheta, \varepsilon_r, \mu_r$ and the flux parameters.

The following auxiliary result, which states the transformation stability with respect to two mesh-dependent norms, will play a key role in the derivation of the desired error estimates.

LEMMA 3.4. *For $\mathbf{E} \in \mathbf{V}(\mathcal{T}_h)$, we have*

$$(3.30) \quad \begin{aligned} \|\mathbf{E}\|_{\mathcal{F}_h} &\leq \rho^{1/2} m_{\text{mid}}^{-\frac{1}{2}} m_{\text{min}}^{-\frac{1}{2}} (1 + \|\Lambda^{\frac{1}{2}}\|^{-1}) \|\hat{\mathbf{E}}\|_{\hat{\mathcal{T}}_h}, \\ \|\mathbf{E}\|_{\mathcal{F}_h^+} &\leq \rho^{1/2} m_{\text{mid}}^{-\frac{1}{2}} m_{\text{min}}^{-\frac{1}{2}} (1 + \|\Lambda^{\frac{1}{2}}\|^{-1}) \|\hat{\mathbf{E}}\|_{\hat{\mathcal{T}}_h^+}. \end{aligned}$$

Proof. We divide the proof into three steps.

Step 1: To estimate $\|[\mu^{-1}\nabla_h \times \mathbf{E}]_T\|_{0,\mathcal{F}_h^I}$ and $\|\mathbf{n} \times (\mu^{-1}\nabla_h \times \mathbf{E})\|_{0,\mathcal{F}_h^B}$.

By the first equation of (3.10) and the first equation of (3.13), we can verify that

$$(3.31) \quad \mu^{-1}\nabla_h \times \mathbf{E} = \mu_r^{-1} P^T \Lambda^{-\frac{1}{2}} \hat{\nabla}_{\hat{h}} \times \hat{\mathbf{E}}.$$

Thus, on the interface $\Gamma_{kj} \in \mathcal{F}_h^I$ we have

$$(3.32) \quad \|[\mu^{-1}\nabla_h \times \mathbf{E}]_T\|_T = \mu_r^{-1} (\mathbf{n}_k \times (P^T \Lambda^{-\frac{1}{2}} \hat{\nabla}_{\hat{h}} \times \hat{\mathbf{E}}_k) + \mathbf{n}_j \times (P^T \Lambda^{-\frac{1}{2}} \hat{\nabla}_{\hat{h}} \times \hat{\mathbf{E}}_j)).$$

It follows by the transformation (3.11) that

$$(3.33) \quad \mathbf{n}_k = |S^{-T} \mathbf{n}_k| S^T \hat{\mathbf{n}}_k = |S^{-T} \mathbf{n}_k| P^T M^T \hat{\mathbf{n}}_k.$$

Notice that $(P^T \mathbf{a}) \times (P^T \mathbf{b}) = P^T (\mathbf{a} \times \mathbf{b})$ ($\forall \mathbf{a}, \mathbf{b} \in R^3$). Then, by (3.33) we obtain

$$(3.34) \quad \begin{aligned} \mathbf{n}_k \times (P^T \Lambda^{-\frac{1}{2}} \hat{\nabla}_{\hat{h}} \times \hat{\mathbf{E}}_k) &= |S^{-T} \mathbf{n}_k| (P^T M^T \hat{\mathbf{n}}_k) \times (P^T \Lambda^{-\frac{1}{2}} \hat{\nabla}_{\hat{h}} \times \hat{\mathbf{E}}_k) \\ &= |S^{-T} \mathbf{n}_k| P^T \left((M^T \hat{\mathbf{n}}_k) \times (\Lambda^{-\frac{1}{2}} \hat{\nabla}_{\hat{h}} \times \hat{\mathbf{E}}_k) \right) = |S^{-T} \mathbf{n}_k| P^T \Lambda^{1/2} \hat{\mathbf{n}}_k \times (\hat{\nabla}_{\hat{h}} \times \hat{\mathbf{E}}_k). \end{aligned}$$

Substituting (3.34) into (3.32), yields

$$(3.35) \quad \|[\mu^{-1}\nabla_h \times \mathbf{E}]_T\|_T = |S^{-T} \mathbf{n}_k| P^T \Lambda^{1/2} \|[\mu_r^{-1} (\hat{\nabla}_{\hat{h}} \times \hat{\mathbf{E}})]_T\|_T.$$

It is easy to see that

$$(3.36) \quad |S^{-T} \mathbf{n}_k| \|\Lambda^{1/2}\| \leq \rho^{1/2},$$

and

$$(3.37) \quad \left(\frac{|\Gamma_{kj}|}{|\hat{\Gamma}_{kj}|} \right)^{\frac{1}{2}} \leq m_{\text{mid}}^{-\frac{1}{2}} m_{\text{min}}^{-\frac{1}{2}}.$$

These, together with (3.35), lead to

$$(3.38) \quad \|[\mu^{-1}\nabla_h \times \mathbf{E}]_T\|_{0,\mathcal{F}_h^I} \leq \rho^{1/2} m_{\text{mid}}^{-\frac{1}{2}} m_{\text{min}}^{-\frac{1}{2}} \|[\mu_r^{-1} \hat{\nabla}_{\hat{h}} \times \hat{\mathbf{E}}]_T\|_{0,\mathcal{F}_h^I}$$

and

$$(3.39) \quad \|\mathbf{n} \times (\mu^{-1}\nabla_h \times \mathbf{E})\|_{0,\mathcal{F}_h^B} \leq \rho^{1/2} m_{\text{mid}}^{-\frac{1}{2}} m_{\text{min}}^{-\frac{1}{2}} \|\hat{\mathbf{n}} \times (\mu_r^{-1} \hat{\nabla}_{\hat{h}} \times \hat{\mathbf{E}})\|_{0,\hat{\mathcal{F}}_h^B}.$$

Step 2: Build estimates of $\|[\mathbf{E}]_T\|_{0,\mathcal{F}_h^I}$ and $\|\mathbf{n} \times \mathbf{E}\|_{0,\mathcal{F}_h^B}$.

By (3.33), the scaling transformation (3.9) and the coordinate transformation (3.11), we obtain

$$(3.40) \quad \mathbf{n}_k \times \mathbf{E}_k = |S^{-T} \mathbf{n}_k| (P^T M^T \hat{\mathbf{n}}_k) \times (P^T \Lambda^{-\frac{1}{2}} \hat{\mathbf{E}}_k).$$

By direct manipulation, we can show that

$$(3.41) \quad \mathbf{n}_k \times \mathbf{E}_k = |S^{-T} \mathbf{n}_k| P^T \Lambda^{1/2} \hat{\mathbf{n}}_k \times \hat{\mathbf{E}}_k.$$

Combining (3.41) with (3.36) and (3.37) yields

$$(3.42) \quad \begin{aligned} \|\llbracket \mathbf{E} \rrbracket_T\|_{0, \mathcal{F}_h^I} &\leq \rho^{1/2} m_{\text{mid}}^{-\frac{1}{2}} m_{\text{min}}^{-\frac{1}{2}} \|\llbracket \hat{\mathbf{E}} \rrbracket_T\|_{0, \hat{\mathcal{F}}_h^I}, \\ \|\mathbf{n} \times \mathbf{E}\|_{0, \mathcal{F}_h^B} &\leq \rho^{1/2} m_{\text{mid}}^{-\frac{1}{2}} m_{\text{min}}^{-\frac{1}{2}} \|\hat{\mathbf{n}} \times \hat{\mathbf{E}}\|_{0, \hat{\mathcal{F}}_h^B}. \end{aligned}$$

Step 3: To estimate $\|\{\{\mathbf{E}\}\}\|_{0, \mathcal{F}_h^I}$, $\|\{\{\mu^{-1} \nabla_h \times \mathbf{E}\}\}\|_{0, \mathcal{F}_h^I}$ and $\|\mathbf{n} \times \mathbf{E}\|_{0, \mathcal{F}_h^B}$.

By the scaling transformation (3.9) and the coordinate transformation (3.11), we get

$$(3.43) \quad \|\{\{\mathbf{E}\}\}\|_{0, \mathcal{F}_h^I} = \|\{\{G \tilde{\mathbf{E}}\}\}\|_{0, \mathcal{F}_h^I} \leq \|G\| \|\{\{\tilde{\mathbf{E}}\}\}\|_{0, \mathcal{F}_h^I} \leq \|\Lambda^{-\frac{1}{2}}\| m_{\text{mid}}^{-\frac{1}{2}} m_{\text{min}}^{-\frac{1}{2}} \|\{\{\hat{\mathbf{E}}\}\}\|_{0, \hat{\mathcal{F}}_h^I}.$$

Moreover, we have

$$(3.44) \quad \begin{aligned} \|\{\{\mu^{-1} \nabla_h \times \mathbf{E}\}\}\|_{0, \mathcal{F}_h^I} &\stackrel{(3.31)}{\leq} \|\{\{\mu_r^{-1} P^T \Lambda^{-\frac{1}{2}} \hat{\nabla}_h \times \hat{\mathbf{E}}\}\}\|_{0, \mathcal{F}_h^I} \\ &\leq \|\Lambda^{-\frac{1}{2}}\| m_{\text{mid}}^{-\frac{1}{2}} m_{\text{min}}^{-\frac{1}{2}} \|\{\{\mu_r^{-1} \hat{\nabla}_h \times \hat{\mathbf{E}}\}\}\|_{0, \hat{\mathcal{F}}_h^I}, \end{aligned}$$

and

$$(3.45) \quad \|\mathbf{n} \times \mathbf{E}\|_{0, \mathcal{F}_h^B} \stackrel{(3.42)}{\leq} \rho^{1/2} m_{\text{mid}}^{-\frac{1}{2}} m_{\text{min}}^{-\frac{1}{2}} \|\hat{\mathbf{n}} \times \hat{\mathbf{E}}\|_{0, \hat{\mathcal{F}}_h^B}.$$

Combining (3.38)-(3.39) with (3.42)-(3.45) gives the desired results (3.30).

□

REMARK 3.1. We point out that, since we have used different choice of G from that in [26], the transformation stability estimates (3.30) with respect to the condition number ρ of Λ are better than (5.7) and (5.8) in [26].

REMARK 3.2. As in the proof of the above Lemma, we can obtain the following transformation stability with respect to two mesh-dependent norms, for $\forall \hat{\mathbf{E}} \in \hat{\mathbf{V}}(\hat{\mathcal{T}}_h)$,

$$(3.46) \quad \begin{aligned} \|\hat{\mathbf{E}}\|_{\hat{\mathcal{F}}_h} &\leq \rho^{1/2} m_{\text{max}}^{\frac{1}{2}} m_{\text{mid}}^{\frac{1}{2}} (1 + \|\Lambda^{-\frac{1}{2}}\|^{-1}) \|\mathbf{E}\|_{\mathcal{F}_h}, \\ \|\hat{\mathbf{E}}\|_{\hat{\mathcal{F}}_h^+} &\leq \rho^{1/2} m_{\text{max}}^{\frac{1}{2}} m_{\text{mid}}^{\frac{1}{2}} (1 + \|\Lambda^{-\frac{1}{2}}\|^{-1}) \|\mathbf{E}\|_{\mathcal{F}_h^+}. \end{aligned}$$

As in [9], we define the following slightly modified weaker norm than L^2 -norm in $\hat{\Omega}$: for every $\hat{\mathbf{v}} \in L^2(\hat{\Omega})^3$,

$$(3.47) \quad \|\hat{\mathbf{v}}\|_{\mathbf{H}(\text{div}; \hat{\Omega})} = \sup_{\hat{\mathbf{u}} \in \mathbf{H}(\text{div}; \hat{\Omega})} \frac{\int_{\hat{\Omega}} \hat{\mathbf{v}} \cdot \hat{\mathbf{u}} \, d\hat{\mathbf{x}}}{\|\hat{\mathbf{u}}\|_{\mathbf{H}(\text{div}; \hat{\Omega})}},$$

where

$$(3.48) \quad \|\hat{\mathbf{u}}\|_{\mathbf{H}(\text{div}; \hat{\Omega})}^2 = \|\hat{\mathbf{v}}\|_{0, \hat{\Omega}}^2 + \|\hat{\nabla} \cdot \hat{\mathbf{v}}\|_{0, \hat{\Omega}}^2,$$

Notice that we have $\|\hat{\mathbf{v}}\|_{\mathbf{H}(\text{div}; \hat{\Omega})} = \|\hat{\mathbf{v}}\|_{0, \hat{\Omega}}$ for every

$$\hat{\mathbf{v}} \in \mathbf{H}(\text{div}^0; \hat{\Omega}) = \left\{ \hat{\mathbf{v}} \in L^2(\hat{\Omega})^3 : \nabla \cdot \hat{\mathbf{v}} = 0 \text{ in } \hat{\Omega} \right\}.$$

Define the following norm: for every \mathbf{w} satisfying $G^{-1}\mathbf{w} \in L^2(\Omega)^3$,

$$(3.49) \quad \|\mathbf{w}\|_{\mathbf{H}(\text{div};\Omega)'} := \sup_{\mathbf{v} \in \mathbf{H}(\text{div};\Omega)} \frac{\int_{\Omega} G^{-1}\mathbf{w} \cdot G^{-1}\mathbf{v} \, d\mathbf{x}}{\|\mathbf{v}\|_{\mathbf{H}(\text{div};\Omega)}}$$

where

$$(3.50) \quad \|\mathbf{v}\|_{\mathbf{H}(\text{div};\Omega)}^2 = \|G^{-1}\mathbf{v}\|_{0,\Omega}^2 + \|\nabla \cdot \mathcal{B}\mathbf{v}\|_{0,\Omega}^2$$

with $\mathcal{B} = \frac{A}{\det^{\frac{1}{2}}(A)}$.

By direct calculation, we have

$$(3.51) \quad \|\nabla \cdot \mathcal{B}\mathbf{v}\|_{0,\Omega}^2 = \|\nabla \cdot \mathcal{B}(G\hat{\mathbf{v}})\|_{0,\Omega}^2 = \|\nabla \cdot (P^T M^{-1}\hat{\mathbf{v}})\|_{0,\Omega}^2 = \det(M^{-1}) \|\hat{\nabla} \cdot \hat{\mathbf{v}}\|_{0,\hat{\Omega}}^2,$$

which yields

$$(3.52) \quad \|\mathbf{v}\|_{\mathbf{H}(\text{div};\Omega)}^2 = \det(M^{-1}) \|\hat{\mathbf{v}}\|_{\mathbf{H}(\text{div};\hat{\Omega})}^2.$$

By the scaling transformation (3.9) and the coordinate transformation (3.11), we obtain the following Lemma.

LEMMA 3.5. For $\mathbf{E} \in \mathbf{V}(\mathcal{T}_h)$, we have

$$(3.53) \quad \|\mathbf{E}\|_{\mathbf{H}(\text{div};\Omega)'} = \det(M^{-1/2}) \|\hat{\mathbf{E}}\|_{\mathbf{H}(\text{div};\hat{\Omega})'}.$$

Proof. By the scaling argument, we have

$$\|\mathbf{E}\|_{\mathbf{H}(\text{div};\Omega)'} \stackrel{(3.49)}{=} \sup_{\mathbf{v} \in \mathbf{H}(\text{div};\Omega)} \frac{\int_{\Omega} G^{-1}\mathbf{E} \cdot G^{-1}\mathbf{v} \, d\mathbf{x}}{\|\mathbf{v}\|_{\mathbf{H}(\text{div};\Omega)}} \stackrel{(3.52)}{=} \sup_{\hat{\mathbf{v}} \in \mathbf{H}(\text{div};\hat{\Omega})} \det(M^{-1/2}) \frac{\int_{\hat{\Omega}} \hat{\mathbf{E}} \cdot \hat{\mathbf{v}} \, d\hat{\mathbf{x}}}{\|\hat{\mathbf{v}}\|_{\mathbf{H}(\text{div};\hat{\Omega})}}.$$

□

With the help of the above preparation, we can prove the final results easily.

THEOREM 3.6. Let \mathbf{E} and \mathbf{E}_h denote the analytical solution of (3.1)-(3.2) and the solution of (3.21), respectively. Suppose that p and r satisfy the conditions in Lemma 3.3. Assume that $\omega\hat{h} \leq C$ and $\mathbf{E} \in \mathbf{H}^{r+1}(\text{curl}; \Omega)$. Then, for sufficiently large p , we have

$$(3.54) \quad \|\mathbf{E} - \mathbf{E}_h\|_{\mathcal{F}_h} \leq C C_2 \rho^{\frac{3}{4}} \omega^{-5/2} \left(\frac{h}{m^{\hat{\lambda}}}\right)^{r-\frac{3}{2}} \|\nabla \times \mathbf{E}\|_{r+1,\omega,\Omega}$$

and

$$(3.55) \quad \|\mathbf{E} - \mathbf{E}_h\|_{\mathbf{H}(\text{div};\Omega)'} \leq C C_3 \rho^{\frac{5}{4}} \omega^{-3} \frac{h^{r-2}}{m^{\hat{\lambda}(r-\frac{3}{2})}} \|\nabla \times \mathbf{E}\|_{r+1,\omega,\Omega},$$

where the constants C_2 and C_3 are defined as

$$C_2 = \|M^{-1}\|^2 (1 + \|A^{\frac{1}{2}}\|^{-1}) \|A^{-\frac{1}{2}}\| \quad \text{and} \quad C_3 = \|M^{-1}\|^3 (1 + \|A^{\frac{1}{2}}\|^{-1}) (1 + \|A^{-\frac{1}{2}}\|).$$

Proof. With the transformations (3.9) and (3.11), we define $\xi_h(\mathbf{x}) = G \hat{\xi}_h(S\mathbf{x})$, where $\hat{\xi}_h$ satisfying (3.29) denotes the plane wave approximation of the scaled electric field $\hat{\mathbf{E}}$. Under

the assumption $\omega \hat{h} \leq C$, we have $C_1(\omega \hat{h}) \leq C$. Thus, by (3.28) and (3.30), together with (3.29), we deduce that

$$(3.56) \quad \begin{aligned} & \|\mathbf{E} - \mathbf{E}_h\|_{\mathcal{F}_h} \leq 3 \|\mathbf{E} - \boldsymbol{\xi}_h\|_{\mathcal{F}_h^+} \leq 3 \rho^{1/2} m_{\text{mid}}^{-\frac{1}{2}} m_{\text{min}}^{-\frac{1}{2}} (1 + \|\Lambda^{\frac{1}{2}}\|^{-1}) \|\hat{\mathbf{E}} - \hat{\boldsymbol{\xi}}_h\|_{\hat{\mathcal{F}}_h^+} \\ & \leq C \rho^{1/2} m_{\text{mid}}^{-\frac{1}{2}} m_{\text{min}}^{-\frac{1}{2}} (1 + \|\Lambda^{\frac{1}{2}}\|^{-1}) \omega^{-5/2} \left(\frac{\hat{h}}{m^\lambda}\right)^{r-\frac{3}{2}} \|\hat{\nabla} \times \hat{\mathbf{E}}\|_{r+1, \omega, \hat{\Omega}}. \end{aligned}$$

By the first equation of (3.10) and the first equation of (3.13), we can deduct that

$$(3.57) \quad (\hat{\nabla} \times \hat{\mathbf{E}})(\hat{\mathbf{x}}) = \Lambda^{-1/2} P (\nabla \times \mathbf{E})(\mathbf{x}).$$

Substituting (3.22) and (3.57) into (3.56), and using the scaling argument, yields

$$(3.58) \quad \begin{aligned} & \|\mathbf{E} - \mathbf{E}_h\|_{\mathcal{F}_h} \leq C \rho^{1/2} m_{\text{mid}}^{-\frac{1}{2}} m_{\text{min}}^{-\frac{1}{2}} (1 + \|\Lambda^{\frac{1}{2}}\|^{-1}) \omega^{-5/2} \left(\frac{\hat{h}}{m^\lambda}\right)^{r-\frac{3}{2}} \|\Lambda^{-1/2} P \nabla \times \mathbf{E}\|_{r+1, \omega, \hat{\Omega}} \\ & \leq C \rho^{1/2} m_{\text{mid}}^{-\frac{1}{2}} m_{\text{min}}^{-\frac{1}{2}} (1 + \|\Lambda^{\frac{1}{2}}\|^{-1}) \omega^{-5/2} \left(\frac{h}{m^\lambda}\right)^{r-\frac{3}{2}} \|M^{-1}\|_{\frac{5}{2}} \|\Lambda^{-\frac{1}{2}}\| (\det(M))^{1/2} \\ & \quad \cdot \|\nabla \times \mathbf{E}\|_{r+1, \omega, \Omega} \leq C C_2 \rho^{\frac{3}{4}} \omega^{-5/2} \left(\frac{h}{m^\lambda}\right)^{r-\frac{3}{2}} \|\nabla \times \mathbf{E}\|_{r+1, \omega, \Omega}. \end{aligned}$$

Furthermore, by (3.53), Proposition 4.8 of [9], (3.22), (3.46) and (3.58), we obtain

$$\begin{aligned} & \|\mathbf{E} - \mathbf{E}_h\|_{\mathbf{H}(\text{div}; \Omega)} \stackrel{(3.53)}{\leq} \det(M^{-1/2}) \|\hat{\mathbf{E}} - \hat{\mathbf{E}}_h\|_{\mathbf{H}(\text{div}; \hat{\Omega})} \\ & \leq C \det(M^{-1/2}) \omega^{-\frac{1}{2}} \hat{h}^{-\frac{1}{2}} \|\hat{\mathbf{E}} - \hat{\mathbf{E}}_h\|_{\hat{\mathcal{F}}_h} \\ & \stackrel{(3.22)}{\leq} C \det(M^{-1/2}) \omega^{-\frac{1}{2}} h^{-\frac{1}{2}} \|M^{-1}\|_{\frac{1}{2}} \|\hat{\mathbf{E}} - \hat{\mathbf{E}}_h\|_{\hat{\mathcal{F}}_h} \\ & \stackrel{(3.46)}{\leq} C \det(M^{-1/2}) \omega^{-\frac{1}{2}} h^{-\frac{1}{2}} \|M^{-1}\|_{\frac{1}{2}} \rho^{1/2} m_{\text{max}}^{\frac{1}{2}} m_{\text{mid}}^{\frac{1}{2}} (1 + \|\Lambda^{-\frac{1}{2}}\|^{-1}) \|\mathbf{E} - \mathbf{E}_h\|_{\mathcal{F}_h} \\ & \stackrel{(3.58)}{\leq} C C_3 \rho^{\frac{5}{4}} \omega^{-3} \frac{h^{r-2}}{m^{\lambda(r-\frac{3}{2})}} \|\nabla \times \mathbf{E}\|_{r+1, \omega, \Omega}. \end{aligned}$$

□

REMARK 3.3. In the considered anisotropic case, the derived error estimates contain a factor depending on the condition number ρ of the coefficient matrix A . In contrast to the shape regularity assumption on \mathcal{T}_h in [26] (where A is a diagonal matrix), we assume that the transformed triangulation $\hat{\mathcal{T}}_h$ is shape regular. Under this assumption, we obtain the important property $\hat{h} \leq C \|M^{-1}\|^{-1} h$ instead of $\hat{h} \leq \|M\| h$ (derived in [26]). By this property, we can build good stabilities of the transformation. Owe to such stabilities, we obtained obviously better error estimates than those in [26, Theorem 5.1] in the sense that the error bounds on the condition number ρ is superior to that of [26]. Besides, we believe that the orders of the condition number ρ in the error estimates are optimal since the transformation stability estimates seem sharp.

4. Numerical experiments. In this Section, we apply the proposed PWDG method to solve the acoustic wave equation and electromagnetic wave propagation in anisotropic media, and we report some numerical results to verify the efficiency of the proposed method.

For Maxwell's equations, we use "new PWDG" to represent the proposed method in this paper, and use "old PWDG" to represent the method introduced in [26], in which the shape regularity assumption was directly imposed on \mathcal{T}_h ([26] only considers the case of the diagonal matrix A). Here, "old PWDG" employs the same variational formulation (3.21) and

coordinate transformation (3.11) as “new PWDG”. For the Helmholtz equation, the formulation of “the old PWDG” is the same as (2.17) of “the new PWDG”, and the only difference between “old PWDG” and “new PWDG” is in a different “shape regularity” assumption on the mesh. As described in Section 2 and Section 3, we choose the same number p of basis functions for every elements Ω_k . We consider the choice of numerical fluxes for the PWDG method as in [6]: the constant parameters $\alpha = \beta = \delta = 1/2$.

To measure the accuracy of the numerical solutions u_h and \mathbf{E}_h , we introduce the following L^2 relative error:

$$\text{err.} = \frac{\|u - u_h\|_{L^2(\Omega)}}{\|u\|_{L^2(\Omega)}}, \quad \text{or} \quad \text{err.} = \frac{\|\mathbf{E} - \mathbf{E}_h\|_{L^2(\Omega)}}{\|\mathbf{E}\|_{L^2(\Omega)}}$$

for the exact solution $u \in L^2(\Omega)$, or $\mathbf{E} \in (L^2(\Omega))^3$. All of the computations have been done in MATLAB, and the system matrix was computed by exact integration on the mesh skeleton. The mesh \mathcal{T}_h of Ω is generated by the Mesh Generation Algorithm of section 2.3.1. We start by covering $\hat{\Omega}$ by a mesh of tetrahedra denoted by $\hat{\mathcal{T}}_h$, which is generated by the software Gmsh [4]. “DOFs” represents the number of degree of freedoms equal to the elements multiplied by the number of basis functions per element.

4.1. The 3D anisotropic Helmholtz equation. The exact solution of the problem is

$$u(\mathbf{x}) = \frac{\exp(i\omega|S \mathbf{x} - \mathbf{x}_0|)}{4\pi|S \mathbf{x} - \mathbf{x}_0|},$$

where $\Omega = [0, 1]^3$. We set the anisotropic matrix $A = \begin{pmatrix} a^2 + \rho^{-1}b^2 & ab(\rho^{-1} - 1) & 0 \\ ab(\rho^{-1} - 1) & b^2 + \rho^{-1}a^2 & 0 \\ 0 & 0 & \rho^{-1} \end{pmatrix}$,

where $a = \frac{1}{\sqrt{2}}$, $b = (1 - a^2)^{\frac{1}{2}} = \frac{1}{\sqrt{2}}$, and $\rho \geq 1$. By orthogonal diagonalizing, we obtain the

diagonal matrix $\Lambda = \text{diag}(1, \rho^{-1}, \rho^{-1})$, and the orthogonal matrix $P = \begin{pmatrix} a & -b & 0 \\ b & a & 0 \\ 0 & 0 & 1 \end{pmatrix}$. Thus,

we have $\|A\| = \|\Lambda\| = 1$, and the condition numbers of the anisotropic matrix $A = P^T \Lambda P$ and the coordinate transformation matrix $S = \Lambda^{-\frac{1}{2}} P$ are ρ and $\rho^{\frac{1}{2}}$, respectively. To keep the exact solution smooth in Ω , we choose the singularity \mathbf{x}_0 as $\mathbf{x}_0 = (-0.6, -0.6, -0.6)$ satisfying $\mathbf{x}_0 \neq S \mathbf{x}$ where $\forall \mathbf{x} \in \Omega$.

First, Table 1 and Figure 2 show the errors of the approximations generated by the proposed PWDG method with respect to m . Here, we set $\omega = 4\pi$, $\rho = 4$, choose the number p of basis functions from $p = 9$ to $p = 64$ ($2 \leq m \leq 7$), and fix the mesh triangulation.

TABLE 1

Errors of the approximations for the case of p -convergence.

p	9	16	25	36	49	64	81
err.	7.61e-1	1.65e-1	2.07e-2	3.23e-3	5.12e-4	8.12e-5	1.46e-5

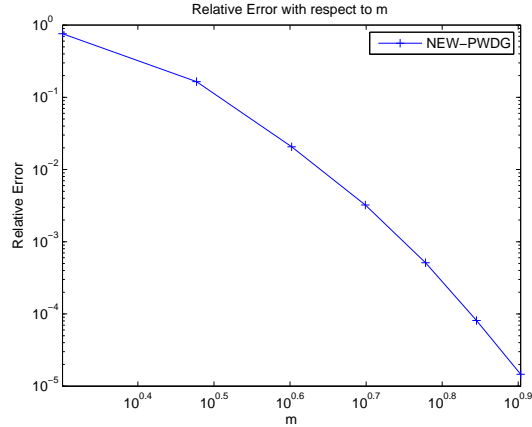
FIG. 2. *Err. vs m.*

Figure 2 shows the plot of L^2 relative errors with respect to m . It highlights two different regimes for increasing m : (i) a preasymptotic region with slow convergence, (ii) a region of faster convergence. **The conclusion is consistent with Figures 4.2-4.5 of [6].**

Then, we would like to compare the L^2 relative errors of the approximations generated by the proposed PWDG method and the old PWDG method in [26] for the case of almost the same degree of freedoms (DOFs). We fix $\omega = 4\pi$, $p = 25$, $\hat{h} = \frac{1}{4}$, but increase the condition number of the anisotropic matrix A and the corresponding number of elements. The numerical results are shown in Table 2 and Figure 3.

TABLE 2
Comparisons of errors of approximations with respect to ρ .

	ρ	8	16	32	64	128	256
old PWDG	err	8.72e-2	2.46e-1	4.55e-1	7.54e-1	1.46	—
	DOFs	12800	25000	54925	102400	200000	390625
new PWDG	err	1.79e-2	2.52e-2	2.86e-2	3.86e-2	5.61e-2	8.02e-2
	DOFs	14400	25600	52900	102400	193600	409600

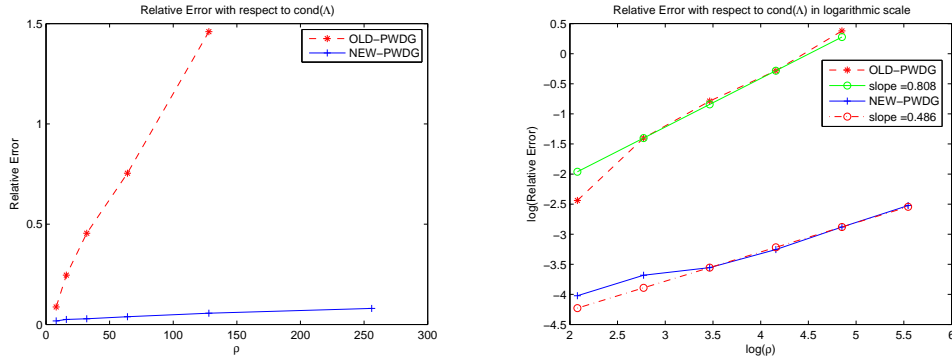


FIG. 3. *Left: Err. vs ρ . Right: Err. vs ρ in logarithmic scale.*

We can see from Table 2 and Figure 3 that, the approximations generated by the new

PWDG are more accurate than those generated by the old PWDG. Besides, **the growth rates with respect to ρ** of the L^2 relative errors of the approximations generated by the new PWDG method are much smaller than those generated by the old PWDG method, which verifies the validity of Remark 2.3. In addition, the numerical convergence order of the approximation u_h generated by the proposed method with respect to ρ is superior to the theoretical convergence order.

Furthermore, we fix the product of $\omega\hat{h}$ to be $\frac{\pi}{2}$, but increase the wave number ω and decrease the mesh size \hat{h} . The resulting errors of the approximations generated by the new PWDG and the old PWDG are listed in Table 3 and Figure 4.

TABLE 3
Comparisons of errors of approximations with respect to ω .

	ω	4π	6π	8π	10π	12π	14π
old PWDG	err	1.23e-3	2.03e-3	3.46e-3	6.16e-3	1.02e-2	1.73e-2
	DOFs	25000	84375	200000	390625	675000	1071875
new PWDG	err	6.97e-4	6.99e-4	7.94e-4	9.13e-4	1.05e-3	1.16e-3
	DOFs	25600	86400	204800	400000	691200	1097600

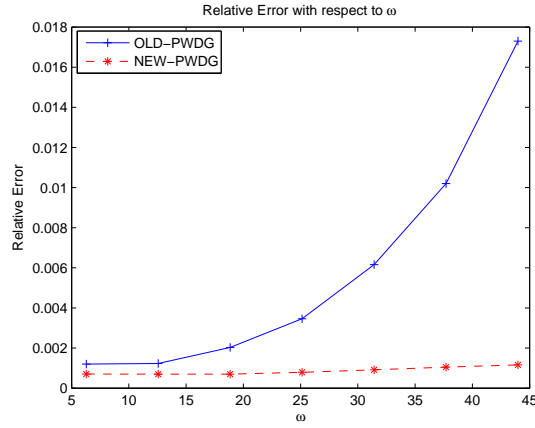


FIG. 4. *Err. vs ω .*

Table 3 and Figure 4 show that, the approximations generated by the new PWDG are more accurate than those generated by the old PWDG. Besides, the numerical errors in relative L^2 norm indicate that the proposed PWDG method is slightly affected by the pollution effect (see [28]).

4.2. Electric dipole in free space for a smooth case. We compute the electric field due to an electric dipole source at the point $\mathbf{x}_0 = (-0.6, -0.6, -0.6)$. The dipole point source can be defined as the solution of a homogeneous Maxwell system (3.1). The exact solution of the problem is

$$(4.1) \quad \mathbf{E}_{\text{ex}} = -i\omega I\phi(\mathbf{x}, \mathbf{x}_0)G \mathbf{a} + \frac{I}{i\omega\epsilon_r}G \nabla_{\hat{h}}(\nabla_{\hat{h}}\phi \cdot \mathbf{a})$$

where

$$\phi(\mathbf{x}, \mathbf{x}_0) = \frac{\exp(i\omega \sqrt{\varepsilon_r} |S \mathbf{x} - \mathbf{x}_0|)}{4\pi |S \mathbf{x} - \mathbf{x}_0|}$$

and $\Omega = [0, 1]^3$. We set the anisotropic matrix $A = \begin{pmatrix} a^2 + \rho b^2 & ab(\rho - 1) & 0 \\ ab(\rho - 1) & b^2 + \rho a^2 & 0 \\ 0 & 0 & \rho \end{pmatrix}$ and

$\varepsilon_r = \mu_r = 1$, where a, b, ρ are the same as in the previous Subsection. By orthogonal diagonalizing, the diagonal matrix $\Lambda = \text{diag}(1, \rho, \rho)$, and the orthogonal matrix P is the same as in the previous Section. Besides, we have $M = \text{diag}(\rho, \rho^{\frac{1}{2}}, \rho^{\frac{1}{2}})$ and $\|M^{-1}\| = \rho^{-\frac{1}{2}}$. In addition, the condition numbers of the anisotropic matrix $A = P^T \Lambda P$ and the coordinate transformation matrix $S = MP$ are ρ and $\rho^{\frac{1}{2}}$, respectively.

First, Table 4 and Figure 5 show the errors of the approximations generated by the PWDG method with respect to m . Here, we set $\omega = 4\pi$, $\rho = 4$. The number p of basis functions is chosen from $p = 9$ to $p = 64$ ($2 \leq m \leq 7$), and the mesh triangulation is fixed.

TABLE 4
Errors of the approximations for the case of p -convergence.

p	9	16	25	36	49	64
err.	2.22e-1	2.31e-2	3.74e-3	4.74e-4	4.54e-5	4.20e-6

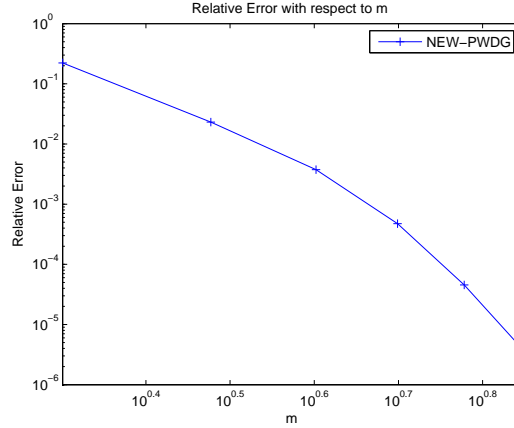


FIG. 5. *Err. vs m.*

Figure 5 shows the plot of L^2 relative errors with respect to m . It also highlights two different regimes for increasing m : (i) a preasymptotic region with slow convergence, (ii) a region of faster convergence. As stated in Remark 3.14 of [6], the convergence order of the approximations with respect to m turns out to be exponential since the analytical solution of the problem can be extended analytically outside the domain.

Next, the L^2 relative errors of the approximations generated by the proposed PWDG method and the old PWDG method in [26] are compared for the case of almost the same DOFs. We fix $\omega = 2\pi$, $p = 25$, $\hat{h} = \frac{1}{2}$, but increase the condition number of the anisotropic matrix A and the corresponding number of elements. The numerical results are shown in Table 5 and Figure 6.

TABLE 5

Comparisons of errors of approximations with respect to ρ .

	ρ	8	16	32	64	128
old PWDG	err	9.42e-2	1.95e-1	4.51e-1	9.09e-1	—
	DOFs	25600	109850	400000	1638400	6632550
new PWDG	err	4.18e-2	6.59e-2	1.14e-1	1.63e-1	2.65e-1
	DOFs	28800	102400	387200	1638400	6771200

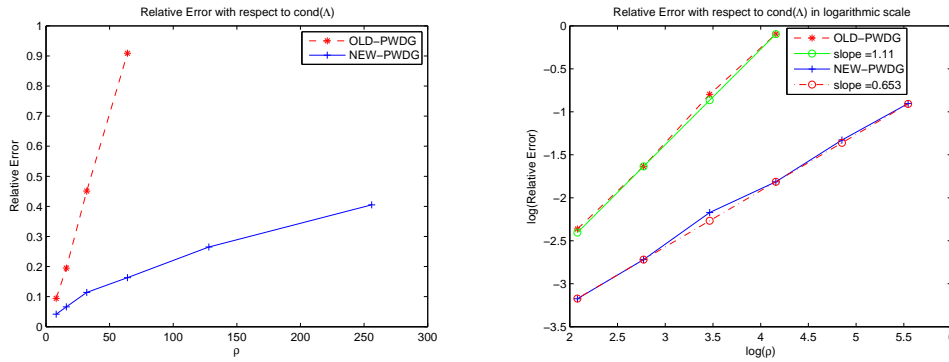


FIG. 6. Left: Err. vs ρ . Right: Err. vs ρ in logarithmic scale.

From Table 5 and Figure 6, we can see that, the approximations generated by the new PWDG are more accurate than those generated by the old PWDG. Moreover, the growth rates with respect to ρ of the L^2 relative errors of the approximations generated by the new PWDG method are much smaller than those generated by the old PWDG method.

Finally, we fix the product of $\omega \hat{h}$ to be $\frac{\pi}{2}$, but increase the wave number ω and decrease the mesh size \hat{h} . The resulting errors of the approximations generated by the new PWDG and the old PWDG are listed in Table 6 and Figure 7.

TABLE 6

Comparisons of errors of approximations with respect to ω .

	ω	3π	4π	5π	6π	7π	8π
old PWDG	err	3.18e-3	3.04e-3	3.78e-3	4.65e-3	6.52e-3	2.28e-2
	DOFs	50000	109850	204800	342950	532400	781250
new PWDG	err	3.04e-3	2.71e-3	2.60e-3	2.56e-3	3.22e-3	3.70e-3
	DOFs	43200	102400	200000	345600	548800	819200

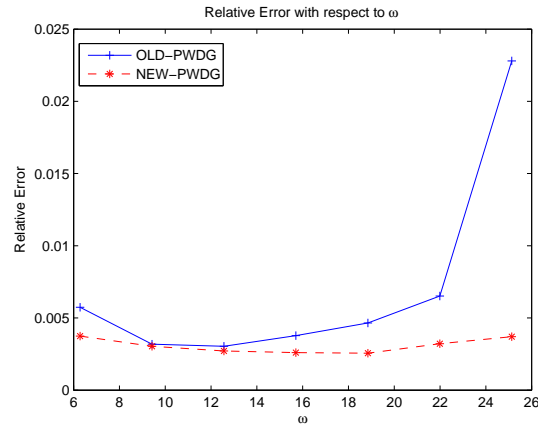
FIG. 7. *Err. vs ω .*

Table 6 and Figure 7 show that, the approximations generated by the new PWDG are more accurate than those generated by the old PWDG. Besides, the numerical errors in relative L^2 norm indicate that the proposed PWDG method is slightly affected by the pollution effect.

Acknowledgments. The authors would like to thank the anonymous reviewer, who gives many insightful comments to improve the presentation of this paper.

REFERENCES

- [1] O. Cessenat, Application d'une nouvelle formulation variationnelle aux équations d'ondes harmoniques, Problèmes de Helmholtz 2D et de Maxwell 3D, Ph.D. Thesis, Université Paris IX Dauphine, 1996.
- [2] O. Cessenat and B. Despres, Application of an ultra weak variational formulation of elliptic pdes to the two-dimensional Helmholtz problem, *SIAM J. Numer. Anal.*, 35(1998), pp. 255-299.
- [3] G. Gabard, Discontinuous Galerkin methods with plane waves for time-harmonic problems, *J. Comput. Phys.*, 225 (2007), pp. 1961-1984.
- [4] C. Geuzaine and J. Remacle, Gmsh: a three-dimensional finite element mesh generator with built-in pre- and post-processing facilities, *Int. J. Numer. Meth. Engng* 79(2009), pp. 1309-1331.
- [5] C. Gittelsohn, R. Hiptmair and I. Perugia, Plane wave discontinuous Galerkin methods: Analysis of the h -version, *ESAIM: M2AN Math. Model. Numer. Anal.*, 43(2009), pp. 297-331.
- [6] R. Hiptmair, A. Moiola, and I. Perugia, Plane wave discontinuous Galerkin methods for the 2D Helmholtz equation: analysis of the p -version, *SIAM J. Numer. Anal.*, 49(2011), pp. 264-284.
- [7] R. Hiptmair, A. Moiola and I. Perugia, Stability results for the time-harmonic Maxwell equations with impedance boundary conditions, *Math. Mod. Meth. Appl. Sci.*, 21(2011), pp. 2263-2287.
- [8] R. Hiptmair, A. Moiola and I. Perugia, Trefftz discontinuous Galerkin methods for acoustic scattering on locally refined meshes, *Appl. Num. Math.*, 79(2013), pp. 79-91.
- [9] R. Hiptmair, A. Moiola, and I. Perugia, Error analysis of Trefftz-discontinuous Galerkin methods for the time-harmonic Maxwell equations, *Math. Comp.*, 82(2013), pp. 247-268.
- [10] R. Hiptmair, A. Moiola and I. Perugia, A survey of Trefftz methods for the Helmholtz equation. In: *Building Bridges: Connections and Challenges in Modern Approaches to Numerical Partial Differential Equations*, Springer International Publishing, (2015), pp. 237-279.
- [11] R. Hiptmair, A. Moiola and I. Perugia, Plane wave discontinuous Galerkin methods: exponential convergence of the hp -version, *Found. Comput. Math.*, 16(2016), pp. 637-675.
- [12] Q. Hu and L. Yuan, A weighted variational formulation based on plane wave basis for discretization of Helmholtz equations, *Int. J. Numer. Anal. Model.*, 11(2014), pp. 587-607.
- [13] Q. Hu and L. Yuan, A Plane Wave Least-Squares Method for Time-Harmonic Maxwell's Equations in Absorbing Media, *SIAM J. Sci. Comput.*, 36(2014), pp. A1911-A1936.
- [14] Q. Hu and L. Yuan, A Plane wave method combined with local spectral elements for nonhomogeneous

- Helmholtz equation and time-harmonic Maxwell equations, *Adv. Comput. Math.*, 44(2018), pp. 245-275.
- [15] T. Huttunen, M. Malinen, P. Monk, Solving Maxwell's equations using the ultra weak variational formulation, *J. Comput. Phys.*, 223 (2007), pp. 731-758.
 - [16] T. Huttunen and P. Monk, The use of plane waves to approximate wave propagation in anisotropic media, *J. Comput. Math.*, 25(2007), pp. 350-367.
 - [17] L. Imbert-Gerard, F. Vico, L. Greengard and M. Ferrando, Integral equation methods for electrostatics, acoustics, and electromagnetics in smoothly varying anisotropic media, *SIAM J. Numer. Anal.*, 57(2019), pp. 1020-1035.
 - [18] A. Moiola, R. Hiptmair, and I. Perugia, Plane wave approximation of homogeneous Helmholtz solutions, *Z. Angew. Math. Phys.*, 62(2011), pp. 809-837.
 - [19] P. Monk, *Finite Element Methods for Maxwell's Equation*, Oxford University Press, New York, 2003.
 - [20] P. Monk and D. Wang, A least-squares method for the Helmholtz equation, *Comput. Meth. Appl. Mech. Engng.*, 175(1999), pp. 121-136.
 - [21] J. Peng, J. Wang and S. Shu, Adaptive BDDC algorithms for the system arising from plane wave discretization of Helmholtz equations, *Int. J. Numer. Methods Eng.*, 116(2018), pp. 683-707.
 - [22] N. Sloane, Tables of spherical codes (with collaboration of R.H. Hardin, W.D. Smith and others) published electronically at <http://www2.research.att.com/njas/packings>, 2000.
 - [23] E. Trefftz, Ein Gegenstück zum Ritzschen Verfahren, *Sec. Inte. Cong. Appl. Mech.*, (1926), pp. 131-137.
 - [24] L. Yuan, A combined scheme of the local spectral element method and the generalized plane wave discontinuous Galerkin method for the anisotropic Helmholtz Equation, *Appl. Numer. Math.*, 150(2020), pp. 341-360.
 - [25] L. Yuan, The Plane Wave Discontinuous Galerkin Method Combined with Local Spectral Finite Elements for the wave propagation in Anisotropic Media, *Numer. Math. Theor. Meth. Appl.*, 12(2019), pp. 517-546.
 - [26] L. Yuan and Q. Hu, Error analysis of the plane wave discontinuous Galerkin method for Maxwell's equations in anisotropic Media, *Commun. Comput. Phys.*, 25(2019), pp. 1496-1522.
 - [27] L. Yuan, Q. Hu and Hengbin An, Parallel preconditioners for plane wave Helmholtz and Maxwell systems with large wave numbers, *Int. J. Numer. Anal. Model.*, 13(2016), 802-819.
 - [28] L. Zhu and H. Wu, Preasymptotic error analysis of CIP-FEM and FEM for Helmholtz equation with large number, *SIAM J. Numer. Anal.*, 51(2013), pp. 1828-1852.